# Comparison of fused-filament fabrication to direct compression and injection molding in the manufacture of oral tablets

Fuenmayor, Evert; Forde, Martin; Healy, Andrew V; Devine, Declan M; Lyons, John G; McConville, Christopher; Major, Ian

*DOI:*
10.1016/j.ijpharm.2019.01.013


# Comparison of fused-filament fabrication to direct compression and injection molding in the manufacture of oral tablets

Evert Fuenmayor, Martin Forde, Andrew V. Healy, Declan M. Devine, John G. Lyons, Christopher McConville, Ian Major

PII: S0378-5173(19)30047-X
DOI: https://doi.org/10.1016/j.ijpharm.2019.01.013
Reference: IJP 18074

To appear in: *International Journal of Pharmaceutics*

Received Date: 23 November 2018
Revised Date: 9 January 2019
Accepted Date: 11 January 2019

Please cite this article as: E. Fuenmayor, M. Forde, A.V. Healy, D.M. Devine, J.G. Lyons, C. McConville, I. Major, Comparison of fused-filament fabrication to direct compression and injection molding in the manufacture of oral tablets, *International Journal of Pharmaceutics* (2019), doi: https://doi.org/10.1016/j.ijpharm.2019.01.013

# Comparison of fused-filament fabrication to direct compression and injection molding in the manufacture of oral tablets

Evert Fuenmayor [1], Martin Forde [1], Andrew V. Healy [1], Declan M. Devine [1], John G. Lyons [1], Christopher McConville [2] and Ian Major [1]*

[1]*Materials Research Institute, Athlone Institute of Technology, Dublin Road, Athlone, Ireland,* [2]*School of Pharmacy, Institute of Clinical Sciences, College of Medical and Dental Sciences, University of Birmingham, UK*

***** Corresponding author: Tel.: +353-906-48-3084

Fax: +353-906-42-4493

E-mail: imajor@ait.ie

**Short title:** Comparison of oral tablets manufacturing

**Keywords:** 3D printing; injection molding; direct compression; hot-melt extrusion; controlled drug release; oral tablets.

## Abstract

Oral tablets are a convenient form to deliver active pharmaceutical ingredients (API) and have a high level of acceptance from clinicians and patients. There is a wide range of excipients available for the fabrication of tablets thereby offering a versatile platform for the delivery of therapeutic agents to the gastrointestinal tract. However, the geometry of tablets is limited by conventional manufacturing processes. This study aimed to compare three manufacturing processes in the production of flat-faced oral tablets using the same formulation composed of a polymer blend and caffeine as a model drug: fused-filament fabrication (FFF), direct compression (DC) and injection molding (IM). Hot-melt extrusion was used to convert a powder blend into feedstock material for FFF and IM processes, while DC was performed on the powder mixture. Tablets were produced with the same dimensions and were characterised for their physical and dissolution properties. There were statistical differences in the physical properties and drug release profiles of the tablets produced by the different manufacturing processes. DC tablets displayed immediate release, IM provided sustained release over 48 hours, and FFF tablets displayed both release types depending on the printing parameters. FFF continues to demonstrate high potential as a manufacturing process for the efficient production of personalized oral tablets.

## Abbreviations

3D, three-dimensional; API, active pharmaceutical ingredient; DC; direct compression; DSC, differential scanning calorimetry; FFF, fused-filament fabrication; HME, hot melt extrusion; HPLC, high-performance liquid chromatography; IM, injection moulding; MFI, melt flow index; MFR, melt flow rates; PCL, polycaprolactone; PEO, poly (ethylene oxide); PVP-VA, Kollidon VA64; RPM, revolutions per minute; SD, standard deviation; SEM, scanning electron microscopy.

# 1. Introduction

Oral drug delivery is of great importance due to high patient compliance and acceptability as well as being suitable for a broad range of drug compounds (Qiu et al., 2017). After ingestion by the patient, oral tablets are exposed to severe conditions in which the drug must withstand the digestive process and penetrate through the gastrointestinal barrier to the bloodstream (Mitra et al., 2013). Conventional tablets are composed of powder blends of one or more active pharmaceutical ingredients (API) along with protective and functional excipients that undergo direct compression in single or multiple steps into compressed solid cylinders (Qiu et al., 2017). Compressed tablets can also have multiple layers to permit the independent delivery of multiple drugs (Vaithiyalingam and Sayeed, 2010). Several factors govern the successful production of a compressed tablet. Proper powder handling is essential as it is involved in every aspect of tablet production. Powder flow is dependent on interparticle interactions and decreases with increasing cohesiveness of the powder. Particle size is vital to overall tablet quality having influence over powder flow, compressibility, content and weight uniformity, drug release, and dissolution (Virtanen et al., 2010). Compactibility is defined as the ability of a powdered mixture under compression to form a stable tablet (Gad, 2007). Under compaction at high pressure powdered blends forms strong bonds between particles. A stable tablet will maintain such bonds during decompression, while unstable tablets will undergo cracking and crumbling due to elastic recovery (Hiestand, 1997). Due to these prerequisite properties for direct compression, less than 20% of drug compounds are suitable candidates for this type of tablet (Li et al., 2017).

Direct compression as a manufacturing process for the production of tablets offers several advantages. Fewer processing steps and less equipment needed when compared to granulation processes as well as a heatless and dry production process, which increases

product stability. The process also allows for the administration of all classes of therapeutic agents, except proteins and faster release rates than its wet granulated counterparts (Jones, 2016). While direct compression is a well understood, highly repeatable process, it is limited in the type of tablet geometries it can generate. Most tablets are circular solid cylinders with either flat or convex faces, with or without edging. Tablet geometry is a factor that can be harnessed to produce oral tablets with unique properties since surface area and volume of an object is directly linked to shape. For example, donut-shaped oral tablets have demonstrated a zero-order release (Kim, 1995). Other issues is that therapeutic agents are not inherently compactable, so more excipients are required to produce reliable tablets, hence, limiting the drug loading achievable through this process (Jones, 2016). The comparison of drug dosage forms fabricated using hot-melt extrusion and direct compression is not new to the literature (Crowley et al., 2004; Liu et al., 2001; Loreti et al., 2014) and it is in the interest of this body of work to evaluate more innovative hot-melt processing techniques. Injection molding is a hot-melt extrusion based process that can readily produce complex parts to six-sigma accuracy and precision, and there is an established interest in the technology for the production of pharmaceutical dosage forms (Major et al., 2016; Quinten et al., 2009; Zema et al., 2012). It is a manufacturing process involving rapid mold filling under high pressure followed by rapid cooling and part ejection. The injection molding machine is composed of two main sections - a plasticizing unit that melts, conveys and injects thermoplastic material, and mold tooling which cools and shapes the molten thermoplastic into a part. In most instances, injection molding is combined with a twin-screw HME process as a first step in the production of pharmaceutical dosage forms (Boyd et al., 2014; Claeys et al., 2012; Desai et al., 2017; Major et al., 2013; Mc Conville et al., 2012; McConville et al., 2016, 2012; Quinten et al., 2012). Twin-screw HME provides for the better dispersion of API in the polymer matrix than what is provided by the single-screw in an injection molding machine

(Maniruzzaman et al., 2012). However, it is not a requisite to melt process formulations for injection moulding applications. The literature offers examples of direct feeding of powder blends for the manufacture of drug dosage forms via injection moulding (Cuff and Raouf, 1999; Eggenreich et al., 2016), including continuous manufacturing processes (Mascia et al., 2013; Melocchi et al., 2015). The technology is also being investigated for tablet coating applications (Desai et al., 2018a, 2018b; Puri et al., 2018).

Among other technologies evaluated for the fabrication of oral tablets, there is fused-filament fabrication (FFF), a three-dimensional (3D) printing process that requires HME for the fabrication of thermoplastic filament feedstock (Alhnan et al., 2016; Feuerbach et al., 2018; Zema et al., 2017). A stepper motor feeds this filament to an extrusion head consisting of a liquefier (a heated chamber), and a nozzle that deposits molten polymer along a coordinate on the XYZ axis. In general, the range of materials available for non-medical FFF applications is limited, with only thirty materials available commercially compared to over three thousand for the other HME based processes like injection molding (Evans, 2016) and currently, no material has been made commercially available for the FFF of drug products. Researchers have two main approaches to creating drug-loaded filament - impregnation of commercial filament (Goyanes et al., 2015a, 2014; Tagami et al., 2017) and HME production of filament from FFF suitable materials like polyvinyl alcohol (Gioumouxouzis et al., 2017; Goyanes et al., 2016b, 2015c, 2015d; Melocchi et al., 2016) and polylactic acid (Goyanes et al., 2016a; Kempin et al., 2017; Melocchi et al., 2016; Wilson and Mills, 2015). Although several pharmaceutical grade polymers have been extensively evaluated for FFF applications in recent years, further work is required to sufficiently modify suitable polymers for the FFF process so that technology can be expanded to suit a broader range of both drug compounds and clinical indications. Recently we described the utilization of melt-blending to overcome

the inherent restrictions in the FFF process (Fuenmayor et al., 2018), and other researchers are investigating similar avenues (Alhijjaj et al., 2016; Solanki et al., 2018). Despite the technical hurdles, there is a growing interest in the utilization of the technology for pharmaceutical applications (Jamróz et al., 2017; Norman et al., 2017; Prasad and Smyth, 2016). Researchers have investigated the use of the process to make oral dosage forms such as tablets (Beck et al., 2017; Chai et al., 2017; Goyanes et al., 2015b, 2015c, 2014; Long et al., 2017; Okwuosa et al., 2016; Solanki et al., 2018; Verstraete et al., 2018),caplets (Goyanes et al., 2016b, 2015d), among other more intricate geometries, compositions and functions (Genina et al., 2017; Maroni et al., 2017; Melocchi et al., 2015; Sadia et al., 2018). Other than the ready production of tablets with complex shapes, a primary driver for the technology is the possibility of the tailored dosage forms to enable the personalisation of treatment (Konta et al., 2017).

The purpose of this study was to directly compare FFF to both DC and IM in the production of flat-faced oral tablets. Tablets were successfully fabricated via all three manufacturing methods using the same formulation and drug loading. The produced tablets were characterized for their mechanical and thermal properties as well as drug release kinetics. A total of twelve different batches of tablets were obtained, ten batches of FFF tablets made with different printing parameters, one batch of DC tablets produced using standard compression parameters and one batch IM tablets produced using standard molding parameters. These batches of tablets were tested for their dimensional accuracy, weight variation, friability, hardness, surface morphology, thermal and melt-flow properties, drug content uniformity and API release kinetics using media simulating fasting stomach conditions.

# 2. Materials and Methods

## *2.1. Materials*

Polycaprolactone (PCL) in powder form (Capa 6506, average $M_w$=50,000) was obtained from Perstop (Cheshire, UK). Kollidon® VA64 (PVP-VA) was purchased from BASF Ireland (Cork, Ireland). Poly (ethylene oxide) (PEO) (average $M_w$=300,000) in powder form was obtained from Sigma-Aldrich (Arklow, Ireland). The model drug for dissolution studies was USP grade caffeine which was purchased from VWR International (Dublin, Ireland). Table 1 shows the formulation used in this study.

## *2.2. Hot-Melt Extrusion*

All excipients were passed through a 450 µm sieve to obtain equivalent particle sizes and then mixed for 15 minutes at 50 RPM using a Universal Motor Drive 400 (Pharmag GmbH, Hamburg, Germany) attached to a cube mixer. An MP19TC25 APV Baker 19 mm co-rotating twin screw extruder (Newcastle-under-Lyme, UK) equipped with a purpose-built filament forming die was used for the compounding of the filament. The filament die has a conical shaped cavity, narrowing away from the extruder finishing in a circular orifice (diameter 2.30 mm). The processing parameters are detailed in Table 2. The extruded materials were hauled off using a tilted conveyor air cooled Teflon® belt and a counter-rotating belt haul-off with sufficient speed to maintain a filament diameter of 1.75 ± 0.15 mm necessary for the FFF 3D printing process. The filament was granulated using a strand pelletizer SGS 50-E (Reduction Engineering Scheer, Ohio, USA) into 3 mm granules for injection molding. Figure 1 is a process flowchart detailing the flow of materials into the three different processes.

## *2.3. Fused-Filament Fabrication*

A MakerBot Replicator 2X (Makerbot® Industries, New York, USA) 3D printer was used for the production of FFF tablets. The optimal printing conditions of the blend were determined via preliminary trials and kept constant at: extrusion speed (10 mm/s), extruder temperature (150 °C), printing bed temperature (50 °C), extruder travel speed (50 mm/s), number of shells (1), roof and floor thickness (0.5 mm), layer height (0.2 mm) and the raft and support options turned off. Three different printing parameters were varied to evaluate the effect on the drug release and tablet properties. Four different values were chosen for the infill percentage (25 %, 50 %, 75 % and 100 %) and layer height (0.1, 0.2, 0.3 and 0.4 mm). Four infill patterns (linear, diamond, moroccanstar and hexagonal) were considered. Generic FFF values were set at 25 % infill with a linear pattern and 0.2 mm layer height. The breakdown of different printed tablets is displayed in Table 3. The three-dimensional design for the tablet was created using SolidWorks® 2014 (Dassault Systèmes, Waltham, USA) and saved as an STL extension format (Figure 2a). The STL file was opened using the monitor and remote control software suite MakerBot Desktop version 3.5 (Makerbot® Industries, New York, USA).

*2.4 Injection Molding*

Injection molding was carried out on an Arburg™ Allrounder 370 E (Arburg GmbH, Germany) equipped with an Arburg™ 170 injection unit. The required temperature profile was established on the Arburg™ Allrounder 370 E injection molding by means of 5 temperature controllers placed along the length of the barrel with an additional controller used to regulate the temperature at the nozzle. The shot size was determined at a stroke of 22 mm based on the total volume of material necessary per shot to fill all runners, gates and part cavities, values that were obtained via SolidWorks® plastics flow simulator (Dassault Systèmes, France). The injection molding parameters (Table 4) were optimised for the formulation prior to tablet production. A mold was specifically designed to produce tablets

with exact geometry the FFF and DC tablets. Solidworks plastics add-on was used to evaluate the efficiency of different mold designs. Figure 2b depicts the three-dimensional drawing and front view of the final mould design used in this work. Two insert molds were manufactured via SLA printing on a Viper SI2 SLA® system (3D systems GmbH, Darmstadt, Germany) using Somos® GP Plus 14122 (DSM Functional Materials, Netherlands) as a feedstock material for the manufacture of the mold, using a resolution of 0.1 mm. The mold was introduced into a full stainless steel cavity mold, which has two orifices that serve as slots for the attachment of small insert molds.

*2.5 Direct Compression*

The tablet press used was a manual laboratory hydraulic press (Specac Limited, UK) capable of 15 tons of pressure. The die was a hardened stainless steel evacuable pellet die Specac GS03000 (Specac Limited, UK) that produces tablets with a diameter of 13 mm. Approximately 500 mg of powder formulation was accurately weighed on a Sartorius analytical balance (Sartorius, Germany) and fed into the die. This amount of material was demonstrated to produce tablets with a height of 4 mm during preliminary trials.The die and plunger were put on top of the powder, and a 5-ton pressure was applied to the mixture for 30 sec.

*2.6. Melt Flow Indexing*

Melt flow indexing (MFI) was performed to evaluate the rheological properties of the material. The melt flow rates (MFR) were measured using a Zwick Roell Cflow extrusion plastometer with a 2 mm orifice die. All testing was performed with a fixed weight of 2.16 kg following the guidelines of the ASTM standard D1238-13. The temperature range for the test extended from 110 °C up to 160 °C in 10 °C increments.

*2.7. Differential Scanning Calorimetry*

Differential scanning calorimetry (DSC) was employed for thermal characterization of material blends and fabricated tablets, using a TA Instruments DSC 2920 Differential Scanning Calorimeter (Dublin, Ireland). Samples weighed between 8 – 12 mg and were placed in non-hermetical aluminium pans, which were crimped prior to testing with an empty crimped aluminium pan for reference. Each sample was subjected to a heating cycle to remove thermal history consisting of a ramp from room temperature to 300 °C at a rate of 10 °C/min. This was followed by a cooling cycle down to 0 °C at a rate of 5 °C/min. Data recording was activated, and the temperature was ramped at a rate of 10 °C/min until 300 °C was reached.

*2.8 Scanning Electron Microscopy*

Scanning electron microscopy (SEM) was performed on a Mira SEM (Tescan Oxford Instruments, UK) using a range of magnifications to evaluate the surface morphology of the tablets and drug using the secondary electrons function. Tablets from the three different manufacturing processes were snap broken through the transversal plane and cross-sectional areas put under the microscope along with powder from caffeine that was left placed in an oven at 140 °C for 12 min to simulate the thermal conditions that the drug withstand during the HME process. As a first step, the samples were placed on an aluminium stub and were gold coated using Baltec SCD 005 sputter coater (BAL-TEC GmbH, Germany) for 110 sec at 0.1 mBar vacuum before observation.

*2.9. Tablet Hardness*

Each formulation underwent tablet hardness testing according to USP <1217> using a Schleuniger Pharmatron Model 6D Tablet Tester (Solothurn, Switzerland). The tablets were

selected at random with each tablet being placed into the hardness tester and the maximum force-to-break (Newton) was measured. The mean ± standard deviation for each formulation was calculated.

*2.10. Tablet Friability*

In order to determine the physical integrity of tablets, an auto-friability tester PTF E/ER (Pharma Test Apparatebau GmbH, Hainburg, Germany) was utilised. Following the USP standard 32-NF 27, tablets were laid in a sieve and using a soft brush; any dust was removed from them. Then tablets were weighted until their combined weight was equal or greater than 6.5 g and introduced into a drum rotated at a speed of 25 ± 1 RPM for 4 min. Tablets were removed and brushed again to remove any dust and reweighed. The loss in the weight of the tablet is the measure of friability and was calculated by dividing the loss in weight by the initial weight and multiplying in it by a 100:

$$\text{Percentage friability (\%)} = \left(\frac{\text{Loss in weight}}{\text{Initial weight}}\right) \times 100 \qquad (1)$$

*2.11. Drug Release Studies*

Dissolution testing of tablets (n = 6) was performed on Distek dissolution system 2100B with a Distek temperature control system TCS 0200B (Distek Inc., USA) according to USP Dissolution Apparatus I. The dissolution media (900 mL per vessel) was 0.2 M hydrochloric acid, pH 1.2 (37 ± 0.5°C) to mimic the stomach conditions during fasting with the stir rate being 50 RPM. At predetermined time intervals, 5 mL was withdrawn from each vessel and replaced with pre-heated media. The withdrawn samples were filtered through 0.45 µm filter and drug release determined at 272 nm by performing UV spectroscopy using a Shimadzu UV-1280 UV-VIS spectrophotometer which was blanked with a solution of the buffer and dissolved polymers, accordingly to the formulation being tested in order to secure the

detection of caffeine. The dissolution profile was observed from a plot of time versus absorbance.

*2.12. High-Performance Liquid Chromatography*

High-performance liquid chromatography (HPLC) was used to determine the content uniformity of caffeine abiding by the standard USP 28 Uniformity of Dosage units. Ten tablets per manufacturing process were randomly selected, weighed and dissolved in 5 mL of chloroform. The solution was then mixed with methanol until 50 mL was obtained. The solutions were centrifuged and injected into HPLC grade vials using a syringe equipped with Nylon 66 0.2 µm filters. The HPLC equipment was a Waters 1515 Isocratic HPLC pump which was connected to an in-line vacuum degasser, Waters 717plus Autosampler and a Waters 2487 Dual Absorbance Detector. The data were collected and integrated using Empower® Version 2.0 software. The column was a Luna C18(2), 5 µM, 150 x 4.6 mm, equipped with a precolumn Security Guard Cartridge C18, 4.0 x 3.0 mm, (Phenomenex Inc., UK). The mobile phase consisted of water:methanol:glacial acetic acid (69:28:3), which was vacuum filtered through a Nylon 66 0.2 µm filter (Agilent Technologies, Ireland). The flow rate of the mobile phase was 2.0 mL/min with an injection volume of 10 µL.

*2.13. Statistical Analysis*

Data handling and analysis were performed using GraphPad Prism 5 (GraphPad Software Inc., UK). Test data was inputted into the software, and mean, and standard deviation values were calculated for replicate sets of data. The significance threshold was set at 0.05. Error bars represent standard deviation unless otherwise specified in the figure caption. The mean values are presented in the figures in the results section. Multiple comparisons among

subgroups were performed using a Bonferroni post-hoc test to differentiate drug release curves.

# 3. Results and Discussion

*3.1 Manufacturing observations*

This work aimed to directly compare FFF 3D printing of flat-faced oral tablets with the well-established DC approach and a second HME based manufacturing process IM. The same formulation was used for all three processes, and physical, thermal and dissolution properties of the resulting tablets were compared. We previously described the development of this formulation (Fuenmayor et al., 2018) as we set about modifying the properties of Kollidon ® VA64 (vinylpyrrolidone-vinyl acetate copolymer) to increase printability for FFF. By melt-blending with PCL and PEO, we were able to decrease filament brittleness and stiffness sufficiently to print complete batches of flat-faced tablets. Each polymer in this ternary blend has previously been used for the fabrication of oral tablets (Diaf et al., 2012; Eyjolfsson, 2015; Kim, 1998; Ma et al., 2013) but to the best of our knowledge not as a blend. Pestle and mortar were implemented to balance size distribution and reduce the particle size of the powder formulation. A 450 µm sieve was the smallest that could be used successfully. The powder blend was mixed to improve homogeneity and stored in an oven at 40 °C overnight before processing to remove moisture.

For the fabrication of DC tablets, 500 mg powder mix was fed into a compression die to produce each tablet. The resulting tablets were coarse in appearance and to the touch. Particle size distribution for PCL and PEO is 98% < 600 µm and 96% < 841 µm respectively while

caffeine particles are mostly below 420 µm in size (95%). The particle size differences between powders can result in a polydisperse and moderately coarse formulation in which PVP-VA is relatively smaller in particle size (15% < 50 µm 2%>250 µm), resulting in a mixture with poor fluidity and compactability due to variations on the particle size distribution (Eyjolfsson, 2015; Yajima et al., 1996). Only one batch of DC tablets was produced using standard compression parameters to compare to the FFF tablets.

An HME twin-screw compounding process converted the powder formulation into a suitable feedstock for FFF (extrudate filament strand) and IM (pelletized extrudate filament < 3 mm). HME was performed at temperatures below the melting temperature of caffeine (235°C), and therefore the drug should have remained in the crystalline state unless solubilized by the molten polymer blend. Addition of drug during extrusion did not affect extruder torque (Fuenmayor et al., 2018), and melt flow indexing of the polymer blend did not change on drug addition and remained around 10.5 g/10min ± 0.02 at 150°C. Melt flow index data had also previously indicated that FFF nozzle temperature should be set to least at 150°C (Fuenmayor et al., 2018) or higher for this polymer blend formulation as the optimal MFI value for FFF layer deposition should be +10 g/10min (Wang et al., 2018). The nozzle temperature was kept constant throughout printing of all ten batches of FFF tablets with only the specific printing parameters changing between batches. Extrudate filaments were pelletized and then gravity fed to the injection molding machine to mold tablets using a temperature profile similar to HME at first. However, this resulted in short-shots which can

be attributed to too low a melt temperature (Moayyedian et al., 2017). A subsequent trial at higher temperatures (Table 4) produced tablets with excellent surface finish and dimensional accuracy.

*3.2 Physical appearance*

Flat-faced tablets were produced via FFF with different printing parameters to understand the effect of each variable on physical and dissolution properties. Infill percentage defines the inner density of a 3DP part. Infill pattern is the layer deposition arrangement during printing. FFF parts are built by depositing horizontal layers of molten material on top of each other, and the thickness of such layers is called layer height. Figure 3 displays the inner structure of FFF tablets with different infill patterns and infill percentages. Figures 3a-d display parts fabricated using increasing infill percentages (25%, 50%, 75% and 100% respectively) and it is clear the reduction of empty space inside parts as the percentage increases. The diamond infill pattern (Figure 3e) had inner walls meeting at a 90°-degree angle. Tablets with a hexagonal infill pattern (Figure 3f) had the thickest inner walls out of the four infill patterns used in this study. The moroccanstar infill pattern (Figure 3g) was composed of a succession of irregular eight-sided stars and octagons. The linear infill pattern (Figure 3h) had a geometrical organization of inner walls similar to the diamond infill pattern, but the space between them was smaller due to a denser distribution of lines.

The surface morphology differences between the three different processes are evident from SEM scans presented in Figure 4. DC tablets (Figures 4a-c) had a coarse surface with no

clear phase differentiation, and on higher magnification (Figure 4b) monoclinic caffeine is apparent. Sponge-like surfaces appear to be engulfing these drug crystals, and it is assumed that it corresponds to PEO domains (Fuenmayor et al., 2018). Figures 4d-f depict the cross-sectional area of an FFF tablet with 25% infill and 0.2 mm layers. The crisscrossing of deposited layers and the space between them is observable in this picture, and the presence of crystalline caffeine more homogenously distributed. Spongy domains in FFF tablets are observed in Figure 4f with a more pronounced colour difference than those in Figure 4b for the DC tablet. The cross-sectional area of tablets fabricated using 100% infill (FFF4) are depicted next (Figures 4g-i). Here it is observable the difference in material density when compare to FFF1 with a compact solid structure, however, evidence of horizontal layer deposition is found in Figure 4g. Drug crystals are only observable when closely inspecting Figure 4i and there seems to be a more chaotic distribution of the material phases when compared to other samples. The SEM images of the IM tablets are displayed in Figures 4j-l. Drug crystals are present but are not as pronounced as those found in the FFF1 and DC tablets, and the crystals are more evenly distributed than in the other three tablets. Figures 4m-o are images of the unprocessed caffeine powder, which shows a less pronounced monoclinic structure compared to the processed caffeine within the tablets, which have more a needle-like appearance, particularly in the FFF tablets. Conclusions about the inner morphological structure of the tablets can be drawn based on these images. Compressed tablets depend on particle bonding and area of contact, plastic deformation and tensile properties to guarantee physical integrity and a successful production process (Jivraj et al.,

2000). Differences in particle size, agglomeration and poor tensile properties could explain the observed lack of surface homogeneity for Figures 4a-c. Conversely, during melt processing, polymer chains are disentangled by means of heat and shear forces (Li et al., 2014), and they are rearranged while the material melt is cooling down which results in a more homogenous continuous inner structure as observable in Figures 4d-i.

*3.3 Physical properties*

The variations in weight between FFF samples were evaluated, and the results are presented in Figure 5. Infill percentage had a greater influence on tablet weight, and this is to be expected since infill percentage increases the amount of material deposited. However, there was no significant difference in the weight of 75% (FFF3) and 100% (FFF4) infill tablets ($p < 0.01$). For the infill pattern, only linear (FFF1) and moroccanstar (FFF5) had no significant difference in their weight ($p < 0.01$), while tablets produced with different layer heights showed no significant ($p < 0.05$) difference between the four tablets (FFF1, FFF8, FFF9 and FFF10). The weight comparison of tablets produced using different manufacturing methods is presented in Figure 6. The differences in tablet weights are significant ($p < 0.01$). The higher weight of IM tablet is a consequence of parts produced using this technique having a considerably higher density (Rothen-Weinhold et al., 1999). FFF tablets have a greater free volume within the inner structure due to the infill percentage used for their fabrication (25%). Even the FFF4 tablet with the highest infill (100%) produced in this study had a lower weight

than the IM tablet, which is an indication of the matrix porosity differences between samples produced using these methods (Verstraete et al., 2018).

As for the tablets physical integrity, all FFF tablets retained their full weight after the friability test. Only DC tablets failed the friability test, and this again could be explained through the differences in particle size of components. Future studies should modify the formulation for the compression of tablets or achieve a more homogenous particle size distribution to improve the compactability of the formulation. Results of tablet hardness for FFF tablets are depicted in Figure 7. Infill percentage seems to have the most substantial effect on tablet hardness, with FFF3 (75%) and FFF4 (100%) exceeding the maximum limit of the test. There was no significant difference between these tablets and FFF2 (50%). Layer height again had no significant effect on tablet hardness. Infill pattern had a significant effect on tablet hardness. The more symmetrical patterns of linear (FFF1), hexagonal (FFF6) and diamond (FFF7) provided greater resistance to the compression forces. The irregular inner geometry of the moroccanstar (FFF5) could explain its poorer mechanical performance since more regular lattice-type structures have a greater load-bearing capacity (Rosen et al., 2006). Tablet hardness of the three different manufacturing processes can be found in Figure 8. The IM tablets failed to deform or break during this test, while the DC tablets needed 176.73 N to break and crumbled apart during testing. Although FFF tablets had the lowest hardness value, they only deformed during testing and did not chip or break apart.

*3.4 Thermal properties*

Figure 9 shows the DSC thermograms for tablets manufactured using three different manufacturing processes. A single melting peak is observed for all polymer blends followed by a relaxation of around 100 °C which corresponds to the PVP-VA glass transition. The temperatures of the transitions observed in Figure 9 are reported in Table 5. The presence of separate transitions in a ternary blend formulation would suggest only partial miscibility between the excipients (Mofokeng and Luyt, 2015), and further data in our previous study of this polymer blend formulation would suggest this to be the case (Fuenmayor et al., 2018). The presence of caffeine was observed for DC tablets by a small melting peak at 240 °C but was not observed for the FFF and IM tablets. The absence of a DSC peak could because the drug was more evenly dispersed in the polymer matrix (as shown by the SEM images) or even partially solubilized during HME (Alshahrani et al., 2015; Huang and Dai, 2014). Another possibility could be the creation of a solid amorphous dispersion during the melt-processing stage of this project (Sarode et al., 2013).

*3.5 Drug release*

Figure 10 shows the drug content uniformity for FFF, DC and IM tablets. DC tablets had a 118.0 % drug content when compared to the label claim with a standard deviation of 16.6 %. Thus, failing to pass the USP uniformity of content test. Conversely, both FFF and IM tablets passed the test with drug contents of 103.9 % (SD = 8.7 %) and 98.2 % (SD = 5.7 %) respectively. The content uniformity difference between DC tablets and the other two tablet types is related to the better drug dispersion and enhanced mixing due to the twin-screw HME processing step before both IM and FFF tablet manufacture (Maniruzzaman et al., 2012;

Thiry et al., 2015). The powder formulations were carefully handled and mixed before the DC process, but there is a possibility for the mixture not to be homogenous, due to the large variation in particle size of the ingredients, causing variations in the actual content of DC tablets. The HME processing step can be added prior to direct compression to improve drug content uniformity. Compressed tablets have previously been formed from the milled powder or granules of melt-extruded blends (Andrews et al., 2008; Lakshman et al., 2011; Liu et al., 2001; Verstraete et al., 2016a). Similarly, Baronsky-Probst et al. (Baronsky-Probst et al., 2016) described the production of tamper-resistant prolonged release tablets made by the direct compaction of melt-extruded rods.

The influence of FFF parameters and manufacturing processes on the drug dissolution properties of oral tablets in fasted stomach conditions was evaluated *in vitro.* Layer height influence on drug delivery is shown in Figure 11. Tablets produced with 0.3 mm (FFF9) and 0.4 mm (FFF10) layer heights released 88% and 92% drug content after 24 hrs respectively. This prolonged release of the drug is hypothesized to be related to the permeability and porosity of tablets. Reducing the layer height creates a more tortuous arrangement over the same volume, slowing the rate of media flushing through the dosage form, thus delaying the drug release (Crowley et al., 2004). Tablets manufactured using 0.2 mm (FFF1) layers provided slower release with only 45% released after 8 hrs. The difference in drug release for all three groups was not significant after the 8 hrs time point ($p > 0.05$), which is due to the release media having imbibed into the tablets negating the differences in permeability

and porosity, while FFF9 and FFF10 were not significantly different from each other ($p > 0.05$) over the 48 hrs.

Drug release properties for tablets fabricated using different infill patterns is presented in Figure 12. There was no clear difference between the three infill patterns in the first 8hrs. Linear (FFF1), moroccanstar (FFF5) and diamond (FFF7) did not display a significant difference in drug release up to 8 hrs. After this point, there was a clear divergence between linear (FFF1) and the moroccanstar (FFF5) and diamond (FFF7) tablets, with the linear (FFF1) tablets releasing more than 90% of their drug content after 48 hrs while the other two tablets released just over 70% in the same time. Release from the hexagonal (FFF6) tablet was not significantly different to the diamond (FFF7) tablet.

Infill percentage has previously been demonstrated to have an inverse relationship to drug release (Verstraete et al., 2018), and similar results were obtained during this study (Figure 13). A higher infill percentage will decrease the inner porosity of tablets which in return will decrease the permeability of the media. Samples fabricated using 75% infill (FFF3) had the slowest release rate with only 26% drug content released after 8 hrs, while 50% infill tablets (FFF2) released 32% of drug content at this time point. After 24 hrs drug release for these tablets increased to 50% for 75 % infill (FFF3) and 61% for 50 % infill (FFF2).

Figure 14 shows the cumulative drug release for the tablets produced using the three different manufacturing processes. DC tablets had burst release characteristics with 95% of drug content present in the media after 6 hrs. The FFF tablet provided a more sustained release with 38% and 80% released after 6 and 24 hrs respectively. After 48 hrs the FFF tablet released 92% drug content. The IM tablet would be considered an extended-release tablet displaying the slowest drug release (64% after 48 hrs) for samples evaluated in this study. During HME, materials are softened and/or melted while having to withstand high shear forces. This generates high pressures compacting the mixture and intertwining the molecular chains of the polymers creating a highly tortuous structure and reducing the porosity of the materials (Crowley et al., 2004; Rubio and Ghaly, 1994; Zhang et al., 2001) This combination of factors explain the sustained release displayed by the tablets produce via FFF and IM. IM had the highest weight of all samples produced, which suggest a highly dense matrix (Rothen-Weinhold et al., 1999). In work by Verstraete et al. (Verstraete et al., 2018, 2016a, 2016b), it was demonstrated the higher porosity of IM tablets when compared to FFF tablets. The increased porosity accelerates the drug release via two methods, the first is facilitating access of dissolution media through the tablet (González-Rodríguez et al., 2003) and the second is by enhancing the diffusion of solubilized drug molecules (Nerurkar et al., 2005).

The differences in porosity are observable when comparing SEM scans of FFF tablets versus IM counterparts (Figure 4d, Figure 4g and Figure 4j). In Figure 4d, there is an abundance of free space as a result of the geometrical pattern used for depositing the material as well the

thickness of horizontal layers used in the building process. Figure 4j in contrast, displays a more compact and multifaceted surface morphology, resembling a single wall of material instead of an arrangement of individual layers. Samples manufactured using 100% infill are dense and solid, and when comparing images of FFF4 versus IM tablets, the resemblance in their wavelike surface finish is appreciable. Nonetheless, as we increased the magnification of the images, the differences in their material density and porosity start arising. A quick glance of Figure 4l, when compared to Figure 4i, shows a more robust wall of material to prevent ingress of the dissolution media into the samples, thus slowing the diffusion of the drug. It is worth mentioning, that DC tablets dissolved fully in the media while all melt-processed tablets held their physical shape and had a mass loss of 30% from their initial weight before dissolution, corresponding to the hydrophilic portions of the formulation (data not shown).

Using the same formulation but different processing methods produce different drug release profiles. However, there is evidence that the hot-melt processes delay drug release (Zhang et al., 2001). The influence of FFF parameters and manufacturing processes on the in vitro drug dissolution properties of oral tablets was tested in fasting stomach conditions. Figure 11 to Figure 13 demonstrate that different FFF parameters did affect the drug release properties. As for infill patterns, there was no significant difference between FFF5 (morrocanstar) and FFF7 (diamond); and FFF1 (linear) did not display a significant difference in its drug release

up to 8 hr. Although FFF6 (hexagonal) had a more rapid release during the first 8 hr, the total amount released was similar to that of FFF5 and FFF7 (data not shown), and only FFF1 delivered more than 90% of its drug content after 48 hrs. Only the linear infill pattern provided significantly different drug release to the other infill patterns.

There were three different drug release profiles for the tablets across manufacturing processes. A burst release was observed for DC tablets, while a more controlled drug release was observed for tablets fabricated using melt processing methods. During the melt processing step needed to prepare samples for FFF and IM, materials are softened and/or molten while being subjected to shear along the barrel. The process generates high pressures compacting the mixture and intertwining the molecular chains of the polymers creating a highly tortuous structure and reducing the porosity of the materials when compared to samples obtained via compression (Crowley et al., 2004; Rubio and Ghaly, 1994; Zhang et al., 2001). This phenomenon is observable via SEM images of the cross-sectional area of tablets as well in the improved physical properties of the tablets when in comparison to DC tablets. This combination of factors explains the extended release kinetics displayed by the tablets produce via FFF and IM.

## 4. Conclusions

New manufacturing technologies are being harnessed by the pharmaceutical industry to produce solid dosage forms. Hot-melt extrusion has been a key enabling technology to enhance drug solubility and bioavailability. Two HME based processes - injection molding and fused-filament fabrication are gaining interest as they both offer a means of producing complex dosage forms that cannot be readily made through more conventional means. This present study has clearly demonstrated tablets of the same physical dimensions and formulation can have very different physical and dissolution properties based on how they are produced. Each process has their advantages and disadvantages. DC has low capital investment and can better handle thermally labile drug compounds, but as we have demonstrated the excipients must have the correct powder properties to produce tablets within the USP limits. The substantially higher capital investment IM process readily manufactures complex shapes to tight tolerances, and we have also shown the process produces densely packed oral tablets with highly dispersed API with extended-release profiles. Although, a much slower process than both DC and IM, the 3D printing process fused-filament fabrication has demonstrated a greater ability to control drug release and tablet properties through simple adjustment of the printing parameters. By modifying layer height and infill percentage, it was possible to modify 24 hr drug release from 92% down to 50% without any changes to infrastructure, formulation or equipment. This kind of flexibility could make 3D printing process the key enabling technology for the modification of drug dosage forms for personalized treatment.

## Acknowledgements

The work was supported by an AIT President's Seed Fund grant and funding from the Technological Higher Education Association Ireland.

## Transparency declarations

The authors declare no conflicts of interest.

# References

Alhijjaj, M., Belton, P., Qi, S., 2016. An investigation into the use of polymer blends to improve the printability of and regulate drug release from pharmaceutical solid dispersions prepared via fused deposition modeling (FDM) 3D printing. Eur. J. Pharm. Biopharm. 108, 111–125. https://doi.org/10.1016/j.ejpb.2016.08.016

Alhnan, M.A., Okwuosa, T.C., Sadia, M., Wan, K.W., Ahmed, W., Arafat, B., 2016. Emergence of 3D Printed Dosage Forms: Opportunities and Challenges. Pharm. Res. 33, 1817–1832. https://doi.org/10.1007/s11095-016-1933-1

Alshahrani, S.M., Lu, W., Park, J.-B., Morott, J.T., Alsulays, B.B., Majumdar, S., Langley, N., Kolter, K., Gryczke, A., Repka, M. a, 2015. Stability-enhanced Hot-melt Extruded Amorphous Solid Dispersions via Combinations of Soluplus® and HPMCAS-HF. AAPS PharmSciTech 16, 824–834. https://doi.org/10.1208/s12249-014-0269-6

Andrews, G.P., Jones, D.S., Diak, O.A., McCoy, C.P., Watts, A.B., McGinity, J.W., 2008. The manufacture and characterisation of hot-melt extruded enteric tablets. Eur. J. Pharm. Biopharm. 69, 264–273. https://doi.org/10.1016/j.ejpb.2007.11.001

Baronsky-Probst, J., Möltgen, C. V., Kessler, W., Kessler, R.W., 2016. Process design and control of a twin screw hot melt extrusion for continuous pharmaceutical tamper-resistant tablet production. Eur. J. Pharm. Sci. 87, 14–21. https://doi.org/10.1016/j.ejps.2015.09.010

Beck, R.C.R., Chaves, P.S., Goyanes, A., Vukosavljevic, B., Buanz, A., Windbergs, M., Basit, A.W., Gaisford, S., 2017. 3D printed tablets loaded with polymeric nanocapsules: An innovative approach to produce customized drug delivery systems. Int. J. Pharm. 528, 268–279. https://doi.org/10.1016/j.ijpharm.2017.05.074

Boyd, P., Major, I., Wang, W., McConville, C., 2014. Development of disulfiram-loaded vaginal rings for the localised treatment of cervical cancer. Eur. J. Pharm. Biopharm. 88, 945–953. https://doi.org/10.1016/j.ejpb.2014.08.002

Chai, X., Chai, H., Wang, X., Yang, J., Li, J., Zhao, Y., Cai, W., Tao, T., Xiang, X., 2017. Fused Deposition Modeling (FDM) 3D Printed Tablets for Intragastric Floating Delivery of Domperidone. Sci. Rep. 7, 2829. https://doi.org/10.1038/s41598-017-03097-x

Claeys, B., Vervaeck, A., Vervaet, C., Remon, J.P., Hoogenboom, R., De Geest, B.G., 2012. Poly(2-ethyl-2-oxazoline) as matrix excipient for drug formulation by hot melt extrusion and injection molding. Macromol. Rapid Commun. 33, 1701–1707. https://doi.org/10.1002/marc.201200332

Crowley, M.M., Schroeder, B., Fredersdorf, A., Obara, S., Talarico, M., Kucera, S., McGinity, J.W., 2004. Physicochemical properties and mechanism of drug release from ethyl cellulose matrix tablets prepared by direct compression and hot-melt extrusion. Int. J. Pharm. 269, 509–522. https://doi.org/10.1016/J.IJPHARM.2003.09.037

Cuff, G., Raouf, F., 1999. A preliminary evaluation of injection moulding as a tableting technology. Pharm. Technol. Eur. 11, 18–26.

Desai, P.M., Hogan, R.C., Brancazio, D., Puri, V., Jensen, K.D., Chun, J.H., Myerson, A.S.,

Trout, B.L., 2017. Integrated hot-melt extrusion – injection molding continuous tablet manufacturing platform: Effects of critical process parameters and formulation attributes on product robustness and dimensional stability. Int. J. Pharm. 531, 332–342. https://doi.org/10.1016/j.ijpharm.2017.08.097

Desai, P.M., Puri, V., Brancazio, D., Halkude, B.S., Hartman, J.E., Wahane, A. V., Martinez, A.R., Jensen, K.D., Harinath, E., Braatz, R.D., Chun, J.H., Trout, B.L., 2018a. Tablet coating by injection molding technology – Optimization of coating formulation attributes and coating process parameters. Eur. J. Pharm. Biopharm. 122, 25–36. https://doi.org/10.1016/j.ejpb.2017.10.006

Desai, P.M., Puri, V., Brancazio, D., Halkude, B.S., Hartman, J.E., Wahane, A. V., Martinez, A.R., Jensen, K.D., Harinath, E., Braatz, R.D., Chun, J.H., Trout, B.L., 2018b. Tablet coating by injection molding technology – Optimization of coating formulation attributes and coating process parameters. Eur. J. Pharm. Biopharm. 122, 25–36. https://doi.org/10.1016/j.ejpb.2017.10.006

Diaf, K., Bahri, Z. El, Chafi, N., Belarbi, L., Mesli, A., 2012. Ethylcellulose, polycaprolactone, and eudragit matrices for controlled release of piroxicam from tablets and microspheres. Chem. Pap. 66, 779–786. https://doi.org/10.2478/s11696-012-0191-x

Eggenreich, K., Windhab, S., Schrank, S., Treffer, D., Juster, H., Steinbichler, G., Laske, S., Koscher, G., Roblegg, E., Khinast, J.G., 2016. Injection molding as a one-step process for the direct production of pharmaceutical dosage forms from primary powders. Int. J. Pharm. 505, 341–351. https://doi.org/10.1016/j.ijpharm.2016.03.034

Evans, J., 2016. 3D Printing Makes Material Advances. [WWW Document]. Plast. Eng. URL http://read.nxtbook.com/wiley/plasticsengineering/october2016/additive_3dprinting.html (accessed 3.29.18).

Eyjolfsson, R., 2015. Introduction, in: Design and Manufacture of Pharmaceutical Tablets. Elsevier, pp. 1–28. https://doi.org/10.1016/B978-0-12-802182-8.00001-5

Feuerbach, T., Kock, S., Thommes, M., 2018. Characterisation of fused deposition modeling 3D printers for pharmaceutical and medical applications, Pharmaceutical Development and Technology. Taylor & Francis. https://doi.org/10.1080/10837450.2018.1492618

Fuenmayor, E., Forde, M., Healy, A., Devine, D., Lyons, J., McConville, C., Major, I., 2018. Material Considerations for Fused-Filament Fabrication of Solid Dosage Forms. Pharmaceutics 10, 44. https://doi.org/10.3390/pharmaceutics10020044

Gad, S.C., 2007. Pharmaceutical Manufacturing Handbook: Production and Processes, Pharmaceutical Manufacturing Handbook: Production and Processes. https://doi.org/10.1002/9780470259818

Genina, N., Boetker, J.P., Colombo, S., Harmankaya, N., Rantanen, J., Bohr, A., 2017. Anti-tuberculosis drug combination for controlled oral delivery using 3D printed compartmental dosage forms: From drug product design to in vivo testing. J. Control. Release 268, 40–48. https://doi.org/10.1016/j.jconrel.2017.10.003

Gioumouxouzis, C.I., Katsamenis, O.L., Bouropoulos, N., Fatouros, D.G., 2017. 3D printed oral solid dosage forms containing hydrochlorothiazide for controlled drug delivery. J. Drug Deliv. Sci. Technol. 40, 164–171. https://doi.org/10.1016/j.jddst.2017.06.008

González-Rodríguez, M.L., Maestrelli, F., Mura, P., Rabasco, A.M., 2003. In vitro release of sodium diclofenac from a central core matrix tablet aimed for colonic drug delivery. Eur. J. Pharm. Sci. 20, 125–131. https://doi.org/10.1016/S0928-0987(03)00181-7

Goyanes, A., Buanz, A.B.M., Basit, A.W., Gaisford, S., 2014. Fused-filament 3D printing (3DP) for fabrication of tablets. Int. J. Pharm. 476, 88–92. https://doi.org/10.1016/j.ijpharm.2014.09.044

Goyanes, A., Buanz, A.B.M., Hatton, G.B., Gaisford, S., Basit, A.W., 2015a. 3D printing of modified-release aminosalicylate (4-ASA and 5-ASA) tablets. Eur. J. Pharm. Biopharm. 89, 157–162. https://doi.org/10.1016/j.ejpb.2014.12.003

Goyanes, A., Chang, H., Sedough, D., Hatton, G.B., Wang, J., Buanz, A., Gaisford, S., Basit, A.W., 2015b. Fabrication of controlled-release budesonide tablets via desktop (FDM) 3D printing. Int. J. Pharm. 496, 414–420. https://doi.org/10.1016/j.ijpharm.2015.10.039

Goyanes, A., Det-Amornrat, U., Wang, J., Basit, A.W., Gaisford, S., 2016a. 3D scanning and 3D printing as innovative technologies for fabricating personalized topical drug delivery systems. J. Control. Release 234, 41–48. https://doi.org/10.1016/j.jconrel.2016.05.034

Goyanes, A., Kobayashi, M., Martínez-Pacheco, R., Gaisford, S., Basit, A.W., 2016b. Fused-filament 3D printing of drug products: Microstructure analysis and drug release characteristics of PVA-based caplets. Int. J. Pharm. 514, 290–295. https://doi.org/10.1016/j.ijpharm.2016.06.021

Goyanes, A., Robles Martinez, P., Buanz, A., Basit, A.W., Gaisford, S., 2015c. Effect of geometry on drug release from 3D printed tablets. Int. J. Pharm. https://doi.org/10.1016/j.ijpharm.2015.04.069

Goyanes, A., Wang, J., Buanz, A., Martínez-Pacheco, R., Telford, R., Gaisford, S., Basit, A.W., 2015d. 3D Printing of Medicines: Engineering Novel Oral Devices with Unique Design and Drug Release Characteristics. Mol. Pharm. 12, 4077–4084. https://doi.org/10.1021/acs.molpharmaceut.5b00510

Hiestand, E.N., 1997. Principles, tenets and notions of tablet bonding and measurements of strength. Eur. J. Pharm. Biopharm. 44, 229–242. https://doi.org/10.1016/S0939-6411(97)00127-6

Huang, Y., Dai, W.-G., 2014. Fundamental aspects of solid dispersion technology for poorly soluble drugs. Acta Pharm. Sin. B 4, 18–25. https://doi.org/10.1016/j.apsb.2013.11.001

Jamróz, W., Kurek, M., Łyszczarz, E., Brniak, W., Jachowicz, R., 2017. Printing techniques: Recent developments in pharmaceutical technology. Acta Pol. Pharm. - Drug Res. 74, 753–763.

Jivraj, M., Martini, L.G., Thomson, C.M., 2000. An overview of the different excipients useful for the direct compression of tablets. Pharm. Sci. Technolo. Today 3, 58–63. https://doi.org/10.1016/S1461-5347(99)00237-0

Jones, D.S., 2016. FASTtrack: Pharmaceutics - Dosage Form and Design, Antimicrobial Agents and Chemotherapy. Cambridge University Press, Cambridge. https://doi.org/10.1128/AAC.03728-14

Kempin, W., Franz, C., Koster, L.C., Schneider, F., Bogdahn, M., Weitschies, W., Seidlitz, A., 2017. Assessment of different polymers and drug loads for fused deposition modeling of drug loaded implants. Eur. J. Pharm. Biopharm. 115, 84–93.

https://doi.org/10.1016/j.ejpb.2017.02.014

Kim, C.-J., 1998. Effects of Drug Solubility, Drug Loading, and Polymer Molecular Weight on Drug Release from Polyox® Tablets. Drug Dev. Ind. Pharm. 24, 645–651. https://doi.org/10.3109/03639049809082366

Kim, C.-J., 1995. Compressed Donut-Shaped Tablets with Zero-Order Release Kinetics. Pharm. Res. An Off. J. Am. Assoc. Pharm. Sci. 12, 1045–1048. https://doi.org/10.1023/A:1016218716951

Konta, A., García-Piña, M., Serrano, D., 2017. Personalised 3D Printed Medicines: Which Techniques and Polymers Are More Successful? Bioengineering 4, 79. https://doi.org/10.3390/bioengineering4040079

Lakshman, J.P., Kowalski, J., Vasanthavada, M., Tong, W.-Q., Joshi, Y.M., Serajuddin, A.T.M., 2011. Application of melt granulation technology to enhance tabletting properties of poorly compactible high-dose drugs. J. Pharm. Sci. 100, 1553–65. https://doi.org/10.1002/jps.22369

Li, Y., Pang, H., Guo, Z., Lin, L., Dong, Y., Li, G., Lu, M., Wu, C., 2014. Interactions between drugs and polymers influencing hot melt extrusion. J. Pharm. Pharmacol. 66, 148–166. https://doi.org/10.1111/jphp.12183

Li, Z., Zhao, L.J., Lin, X., Shen, L., Feng, Y., 2017. Direct compaction: An update of materials, trouble-shooting, and application. Int. J. Pharm. 529, 543–556. https://doi.org/10.1016/j.ijpharm.2017.07.035

Liu, J., Zhang, F., McGinity, J.W., 2001. Properties of lipophilic matrix tablets containing phenylpropanolamine hydrochloride prepared by hot-melt extrusion. Eur. J. Pharm. Biopharm. 52, 181–190. https://doi.org/10.1016/S0939-6411(01)00162-X

Long, J., Gholizadeh, H., Lu, J., Bunt, C., Seyfoddin, A., 2017. Application of Fused Deposition Modelling (FDM) Method of 3D Printing in Drug Delivery. Curr. Pharm. Des. 23, 433–439. https://doi.org/10.2174/1381612822666161026162707

Loreti, G., Maroni, A., Del Curto, M.D., Melocchi, A., Gazzaniga, A., Zema, L., 2014. Evaluation of hot-melt extrusion technique in the preparation of HPC matrices for prolonged release. Eur. J. Pharm. Sci. 52, 77–85. https://doi.org/10.1016/j.ejps.2013.10.014

Ma, L., Deng, L., Chen, J., 2013. Applications of poly(ethylene oxide) in controlled release tablet systems: a review. Drug Dev. Ind. Pharm. 9045, 1–7. https://doi.org/10.3109/03639045.2013.831438

Major, I., Boyd, P., Kilbourne-Brook, M., Saxon, G., Cohen, J., Malcolm, R.K., 2013. A modified SILCS contraceptive diaphragm for long-term controlled release of the HIV microbicide dapivirine. Contraception 88, 58–66. https://doi.org/10.1016/j.contraception.2012.10.018

Major, I., Fuenmayor, E., Mcconville, C., 2016. The Production of Solid Dosage Forms from Non-Degradable Polymers. urrent Pharm. Des. 22, 2738–2760.

Maniruzzaman, M., Boateng, J.S., Snowden, M.J., Douroumis, D., 2012. A review of hot-melt extrusion: process technology to pharmaceutical products. ISRN Pharm. 2012, 436763–436769. https://doi.org/10.5402/2012/436763

Maroni, A., Melocchi, A., Parietti, F., Foppoli, A., Zema, L., Gazzaniga, A., 2017. 3D printed

multi-compartment capsular devices for two-pulse oral drug delivery. J. Control. Release 268, 10–18. https://doi.org/10.1016/j.jconrel.2017.10.008

Mascia, S., Heider, P.L., Zhang, H., Lakerveld, R., Benyahia, B., Barton, P.I., Braatz, R.D., Cooney, C.L., Evans, J.M.B., Jamison, T.F., Jensen, K.F., Myerson, A.S., Trout, B.L., 2013. End-to-end continuous manufacturing of pharmaceuticals: Integrated synthesis, purification, and final dosage formation. Angew. Chemie - Int. Ed. 52, 12359–12363. https://doi.org/10.1002/anie.201305429

Mc Conville, C., Major, I., Friend, D.R., Clark, M.R., Woolfson, a. D., Malcolm, R.K., 2012. Development of polylactide and polyethylene vinyl acetate blends for the manufacture of vaginal rings. J. Biomed. Mater. Res. - Part B Appl. Biomater. 100 B, 891–895. https://doi.org/10.1002/jbm.b.31919

McConville, C., Major, I., Devlin, B., Brimer, A., 2016. Development of a multi-layered vaginal tablet containing dapivirine, levonorgestrel and acyclovir for use as a multipurpose prevention technology. Eur. J. Pharm. Biopharm. 104, 171–179. https://doi.org/10.1016/j.ejpb.2016.05.003

McConville, C., Major, I., Friend, D.R., Clark, M.R., Malcolm, R.K., 2012. Development of a UC781 releasing polyethylene vinyl acetate vaginal ring. Drug Deliv. Transl. Res. 2, 489–497.

Melocchi, A., Loreti, G., Del Curto, M.D., Maroni, A., Gazzaniga, A., Zema, L., 2015. Evaluation of hot-melt extrusion and injection molding for continuous manufacturing of immediate-release tablets. J. Pharm. Sci. 104, 1971–1980. https://doi.org/10.1002/jps.24419

Melocchi, A., Parietti, F., Maroni, A., Foppoli, A., Gazzaniga, A., Zema, L., 2016. Hot-melt extruded filaments based on pharmaceutical grade polymers for 3D printing by fused deposition modeling. Int. J. Pharm. 509, 255–263. https://doi.org/10.1016/j.ijpharm.2016.05.036

Mitra, A.K., Lee, C.H., Cheng, K., 2013. Advance Drug Delivery, Journal of Chemical Information and Modeling. https://doi.org/10.1017/CBO9781107415324.004

Moayyedian, M., Abhary, K., Marian, R., 2017. The analysis of short shot possibility in injection molding process. Int. J. Adv. Manuf. Technol. 91, 3977–3989. https://doi.org/10.1007/s00170-017-0055-1

Mofokeng, J.P., Luyt, A.S., 2015. Dynamic mechanical properties of PLA/PHBV, PLA/PCL, PHBV/PCL blends and their nanocomposites with TiO2 as nanofiller. Thermochim. Acta 613, 41–53. https://doi.org/10.1016/j.tca.2015.05.019

Nerurkar, J., Jun, H.W., Price, J.C., Park, M.O., 2005. Controlled-release matrix tablets of ibuprofen using cellulose ethers and carrageenans: Effect of formulation factors on dissolution rates. Eur. J. Pharm. Biopharm. 61, 56–68. https://doi.org/10.1016/j.ejpb.2005.03.003

Norman, J., Madurawe, R.D., Moore, C.M.V., Khan, M.A., Khairuzzaman, A., 2017. A new chapter in pharmaceutical manufacturing: 3D-printed drug products. Adv. Drug Deliv. Rev. 108, 39–50. https://doi.org/10.1016/j.addr.2016.03.001

Okwuosa, T.C., Stefaniak, D., Arafat, B., Isreb, A., Wan, K.W., Alhnan, M.A., 2016. A Lower Temperature FDM 3D Printing for the Manufacture of Patient-Specific

Immediate Release Tablets. Pharm. Res. 33, 2704–2712. https://doi.org/10.1007/s11095-016-1995-0

Prasad, L.K., Smyth, H., 2016. 3D Printing technologies for drug delivery: a review. Drug Dev. Ind. Pharm. 42, 1019–1031. https://doi.org/10.3109/03639045.2015.1120743

Puri, V., Brancazio, D., Harinath, E., Martinez, A.R., Desai, P.M., Jensen, K.D., Chun, J.H., Braatz, R.D., Myerson, A.S., Trout, B.L., 2018. Demonstration of pharmaceutical tablet coating process by injection molding technology. Int. J. Pharm. 535, 106–112. https://doi.org/10.1016/j.ijpharm.2017.10.062

Qiu, Y., Chen, Y., Zhang, G.G., Yu, L., Mantri, R. V, 2017. Developing Solid Oral Dosage Forms.

Quinten, T., Andrews, G.P., Beer, T., Saerens, L., Bouquet, W., Jones, D.S., Hornsby, P., Remon, J.P., Vervaet, C., 2012. Preparation and Evaluation of Sustained-Release Matrix Tablets Based on Metoprolol and an Acrylic Carrier Using Injection Moulding. AAPS PharmSciTech 13. https://doi.org/10.1208/s12249-012-9848-6

Quinten, T., Beer, T. De, Vervaet, C., Remon, J.P., 2009. Evaluation of injection moulding as a pharmaceutical technology to produce matrix tablets. Eur. J. Pharm. Biopharm. 71, 145–154. https://doi.org/10.1016/j.ejpb.2008.02.025

Rosen, D., Johnston, S., Reed, M., 2006. Design of General Lattice Structures for Lightweight and Compliance Applications. Rapid Manuf. Conf. 1–14.

Rothen-Weinhold, A., Besseghir, K., Vuaridel, E., Sublet, E., Oudry, N., Kubel, F., Gurny, R., 1999. Injection-molding versus extrusion as manufacturing technique for the preparation of biodegradable implants. Eur. J. Pharm. Biopharm. 48, 113–121. https://doi.org/10.1016/S0939-6411(99)00034-X

Rubio, M.R., Ghaly, E.S., 1994. In-Vitro Release of Acetaminophen from Sodium Alginate Controlled Release Pellets. Drug Dev. Ind. Pharm. 20, 1239–1251. https://doi.org/10.3109/03639049409038364

Sadia, M., Arafat, B., Ahmed, W., Forbes, R.T., Alhnan, M.A., 2018. Channelled tablets : An innovative approach to accelerating drug release from 3D printed tablets. J. Control. Release 269, 355–363. https://doi.org/10.1016/j.jconrel.2017.11.022

Sarode, A.L., Sandhu, H., Shah, N., Malick, W., Zia, H., 2013. Hot melt extrusion (HME) for amorphous solid dispersions: Predictive tools for processing and impact of drug–polymer interactions on supersaturation. Eur. J. Pharm. Sci. 48, 371–384. https://doi.org/10.1016/j.ejps.2012.12.012

Solanki, N.G., Tahsin, M., Shah, A. V., Serajuddin, A.T.M., 2018. Formulation of 3D Printed Tablet for Rapid Drug Release by Fused Deposition Modeling: Screening Polymers for Drug Release, Drug-Polymer Miscibility and Printability. J. Pharm. Sci. 107, 390–401. https://doi.org/10.1016/j.xphs.2017.10.021

Tagami, T., Fukushige, K., Ogawa, E., Hayashi, N., Ozeki, T., 2017. 3D Printing Factors Important for the Fabrication of Polyvinylalcohol Filament-Based Tablets. Biol. Pharm. Bull. 40, 357–364. https://doi.org/10.1248/bpb.b16-00878

Thiry, J., Krier, F., Evrard, B., 2015. A review of pharmaceutical extrusion: Critical process parameters and scaling-up. Int. J. Pharm. 479, 227–240. https://doi.org/10.1016/j.ijpharm.2014.12.036

Vaithiyalingam, S.R., Sayeed, V.A., 2010. Critical factors in manufacturing multi-layer tablets-Assessing material attributes, in-process controls, manufacturing process and product performance. Int. J. Pharm. 398, 9–13. https://doi.org/10.1016/j.ijpharm.2010.07.025

Verstraete, G., Mertens, P., Grymonpré, W., Van Bockstal, P.J., De Beer, T., Boone, M.N., Van Hoorebeke, L., Remon, J.P., Vervaet, C., 2016a. A comparative study between melt granulation/compression and hot melt extrusion/injection molding for the manufacturing of oral sustained release thermoplastic polyurethane matrices. Int. J. Pharm. 513, 602–611. https://doi.org/10.1016/j.ijpharm.2016.09.072

Verstraete, G., Samaro, A., Grymonpré, W., Vanhoorne, V., Van Snick, B., Boone, M.N., Hellemans, T., Van Hoorebeke, L., Remon, J.P., Vervaet, C., 2018. 3D printing of high drug loaded dosage forms using thermoplastic polyurethanes. Int. J. Pharm. 536, 318–325. https://doi.org/10.1016/j.ijpharm.2017.12.002

Verstraete, G., Van Renterghem, J., Van Bockstal, P.J., Kasmi, S., De Geest, B.G., De Beer, T., Remon, J.P., Vervaet, C., 2016b. Hydrophilic thermoplastic polyurethanes for the manufacturing of highly dosed oral sustained release matrices via hot melt extrusion and injection molding. Int. J. Pharm. 506, 214–221. https://doi.org/10.1016/j.ijpharm.2016.04.057

Virtanen, S., Antikainen, O., Räikkönen, H., Yliruusi, J., 2010. Granule size distribution of tablets. J. Pharm. Sci. 99, 2061–2069. https://doi.org/10.1002/jps.21945

Wang, S., Capoen, L., D'hooge, D.R., Cardon, L., 2018. Can the melt flow index be used to predict the success of fused deposition modelling of commercial poly(lactic acid) filaments into 3D printed materials? Plast. Rubber Compos. 47, 9–16. https://doi.org/10.1080/14658011.2017.1397308

Wilson, C.G., Mills, D.K., 2015. Antibiotic and chemotherapeutic enhanced three-dimensional printer filaments and constructs for biomedical applications 357–370.

Yajima, T., Itai, S., Hayashi, H., Takayama, K., Nagai, T., 1996. Optimization of Size Distribution of Granules for Tablet Compression. Chem. Pharm. Bull. (Tokyo). 44, 1056–1060. https://doi.org/10.1248/cpb.44.1056

Zema, L., Loreti, G., Melocchi, A., Maroni, A., Gazzaniga, A., 2012. Injection Molding and its application to drug delivery. J. Control. Release 159, 324–331. https://doi.org/10.1016/j.jconrel.2012.01.001

Zema, L., Melocchi, A., Maroni, A., Gazzaniga, A., 2017. Three-Dimensional Printing of Medicinal Products and the Challenge of Personalized Therapy. J. Pharm. Sci. 106, 1697–1705. https://doi.org/10.1016/j.xphs.2017.03.021

Zhang, Y., Tchao, R., Schwartz, J.B., 2001. Effect of Processing Methods and Heat Treatment on the Formation of Wax Matrix Tablets for Sustained Drug Release. Pharm. Dev. Technol. 6, 131–144. https://doi.org/10.1081/PDT-100000736

**Figure Captions**

**Fig. 1.** Process flow chart detailing the different process steps and flow of materials in this study.

**Fig. 2.** CAD design of a flat-face plain tablet for (a) fused-filament fabrication (b) injection molding (scale 1:2).

**Fig. 3.** 3DP PCL samples of different infill percentages and patterns, (a) 25% infill, (b) 50% infill, (c) 75% infill, (d) 100% infill, (e) Diamond, (f) Hexagonal, (g) Moroccanstar, (h) Linear. 25% infill was used for all different infill patterns. Scale bars represents 1 mm for Figure 3 (c) and Figure 3 (d), for the rest, the bar represents 10 mm.

**Fig. 4.** SEM images of the three tablets and the model drug used in this study at two different magnifications: (a) DC tablet, mag: 100X; (b) DC tablet, mag: 250KX; (c) DC tablet, mag: 1KX; (d) FFF1 (25% infill) tablet, mag: 100X; (e), FFF1 (25% infill) tablet, mag: 250X; (f) FFF1 (25% infill) tablet, mag: 1KX; (g) FFF4 (100% infill), mag: 100X; (h) FFF4 (100% infill), mag: 250X; (i) FFF4 (100% infill), mag: 1KX; (j) IM tablet, mag: 100X; (k) IM tablet, mag: 250X; (l) IM tablet, mag: 1KX; (m) Caffeine, mag: 250X; (n) Caffeine, mag: 1KX; (o) Caffeine, mag: 2.8KX. Scale bars represent, from left to right, 500 µm, 200 µm and 50 µm respectively for all rows of images above except caffeine images (Fig 4 (m), (n) and (o)). Scale bars on Fig 4 (m), Fig 4 (n) and Fig 4 (o) represent 200 µm. 50 µm and 20 µm.

**Fig. 5.** Weight uniformity mean values for all FFF tablets (n = 10).

**Fig. 6.** Weight uniformity mean values for tablets manufactured using three different production methods (n = 10).

**Fig. 7.** FFF tablet hardness (N) values represented in Newton with standard deviation (n = 11).

**Fig. 8.** Tablet hardness values in Newton across three different manufacturing processes (n = 11).

**Fig. 9.** Overlaid DSC thermograms of the model drug caffeine and tablets manufactured in this study.

**Fig. 10.** Uniformity of drug content for tablets manufactured using three different production methods. Horizontal lines represent the ±15% threshold for drug content tolerance (n=10).

**Fig. 11.** Cumulative caffeine release over 48hr in HCl 1.2 pH, 0.2M media for different tablets produced via 3DP with different layer heights and 25% linear infill. FFF1: 0.2 mm, FFF9: 0.3 mm, FFF10: 0.4 mm.

**Fig. 12.** Cumulative caffeine release over 48 hrs in HCl 1.2 pH, 0.2M media for different tablets produced via 3DP with different infill patterns at 25% infill and 0.2 mm layer height. FFF1: linear, FFF5: Moroccanstar, FFF7: Diamond.

**Fig. 13**. Cumulative caffeine release over 48 hrs in HCl 1.2 pH, 0.2M media for different tablets produced via 3DP with different linear infill percentages and 0.2 mm layer height. FFF1: 25% infill, FFF2: 50% infill, FFF3: 75% infill.

**Fig. 14**. Cumulative caffeine release over 48 hrs in HCl 1.2 pH, 0.2M media for different tablets produced via three different manufacturing processes using the same formulation.

**Table 1.**

Formulation profile used in the production of all three tablet types. The values represent the composition by weight as a percentage (w/w)

| PVP-VA (%) | Caffeine (%) | PCL (%) | PEO (%) |
|---|---|---|---|
| 28.5 | 5.0 | 57.0 | 9.5 |

**Table 2.**

Temperature profile in Celsius (°C) for twin-screw compounding HME process to produce filament.

| Zone 1 (°C) | Zone 2 (°C) | Zone 3 (°C) | Zone 4 (°C) | Zone 5 (°C) | Zone 6 (°C) | Flange (°C) | Die (°C) |
|---|---|---|---|---|---|---|---|
| 80 | 90 | 100 | 110 | 120 | 130 | 140 | 140 |

Screw speed: 80 RPM, Feeding rate: 0.4 kg/hr.

**Table 3**.

Different 3D printing parameters used in this body of work for the fabrication of tablets.

| Tablet Name | Infill Percentage | Infill Pattern | Layer Height |
|---|---|---|---|
| FFF1 | 25 % | Linear | 0.2 mm |
| FFF2 | 50 % | Linear | 0.2 mm |
| FFF3 | 75 % | Linear | 0.2 mm |
| FFF4 | 100 % | Linear | 0.2 mm |
| FFF5 | 25 % | Moroccanstar | 0.2 mm |
| FFF6 | 25 % | Hexagonal | 0.2 mm |
| FFF7 | 25 % | Diamond | 0.2 mm |
| FFF8 | 25 % | Linear | 0.1 mm |
| FFF9 | 25 % | Linear | 0.3 mm |
| FFF10 | 25 % | Linear | 0.4 mm |

**Table 4.**

Injection molding manufacturing profile used in this work.

| | Zone 1 | Zone 2 | Zone 3 | Zone 4 | Zone 5 | Nozzle |
|---|---|---|---|---|---|---|
| Temperature (°C) | 30 | 120 | 130 | 140 | 150 | 160 |

Holding time (sec): 6.5; Cooling time (sec): 60; Holding Pressure (bar): 200; Injection Pressure (bar): 450; Back Pressure (bar): 15.

**Table 5**

Observed transitions on DSC thermographs the model drug caffeine and the three different oral tablets

| Sample | Glass transition (°C) | Melting (°C) |
|---|---|---|
| FFF | 108.66 | 66.27 |
| IM | 108.10 | 63.89 |
| DC | - | 66.55\| 214.85 \|240.73 |
| Caffeine | - | 240.89 |

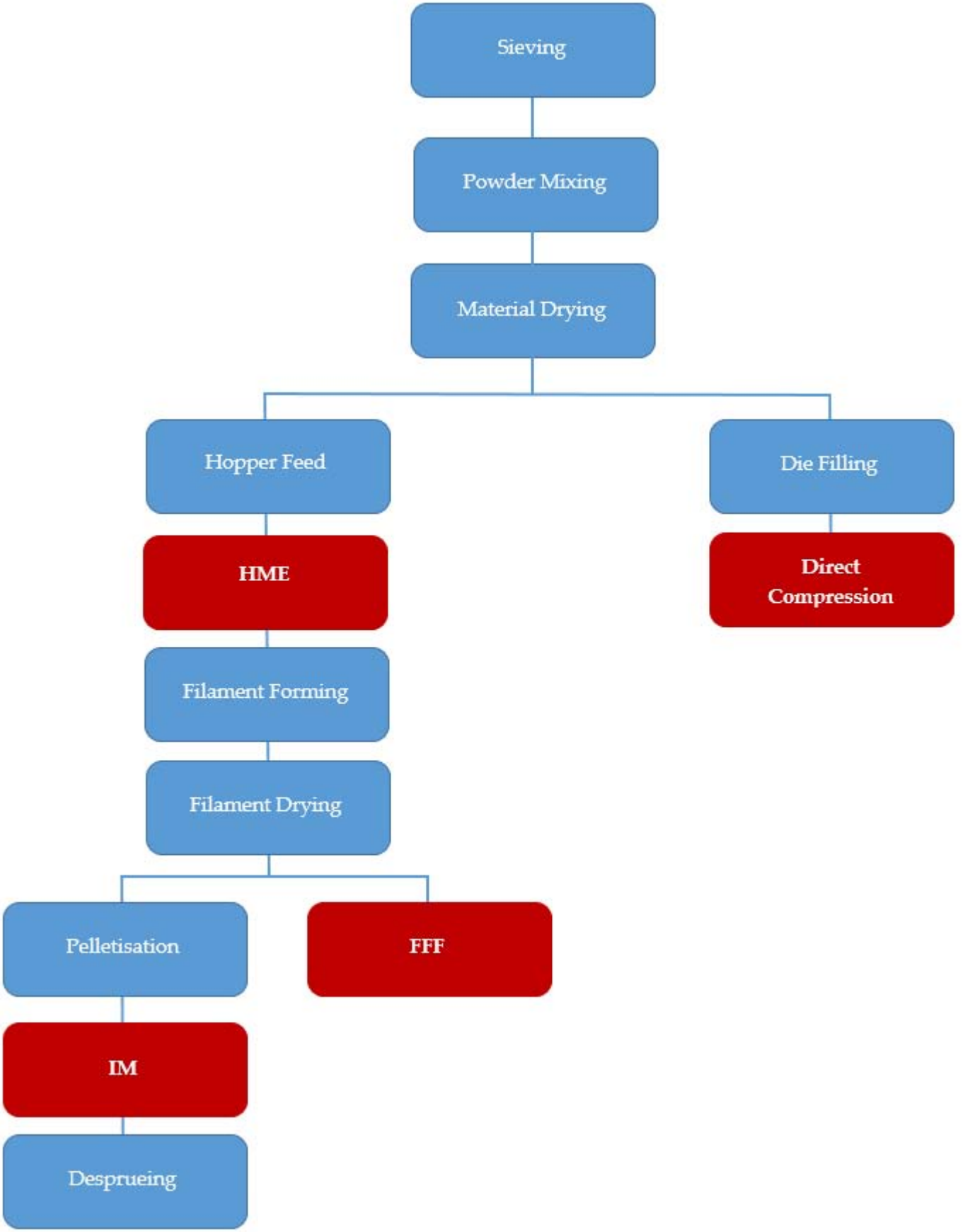
Sieving
Powder Mixing
Material Drying
Hopper Feed
Die Filling
HME
Direct Compression
Filament Forming
Filament Drying
Pelletisation
FFF
IM
Desprueing

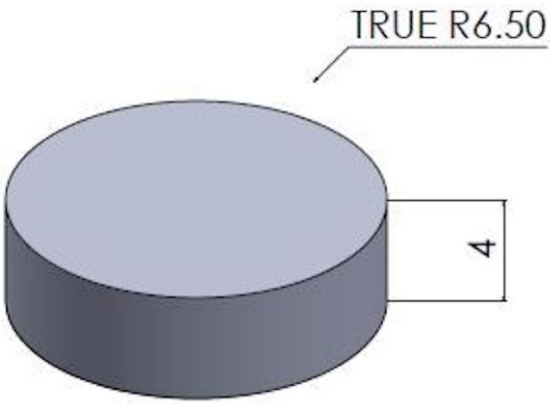


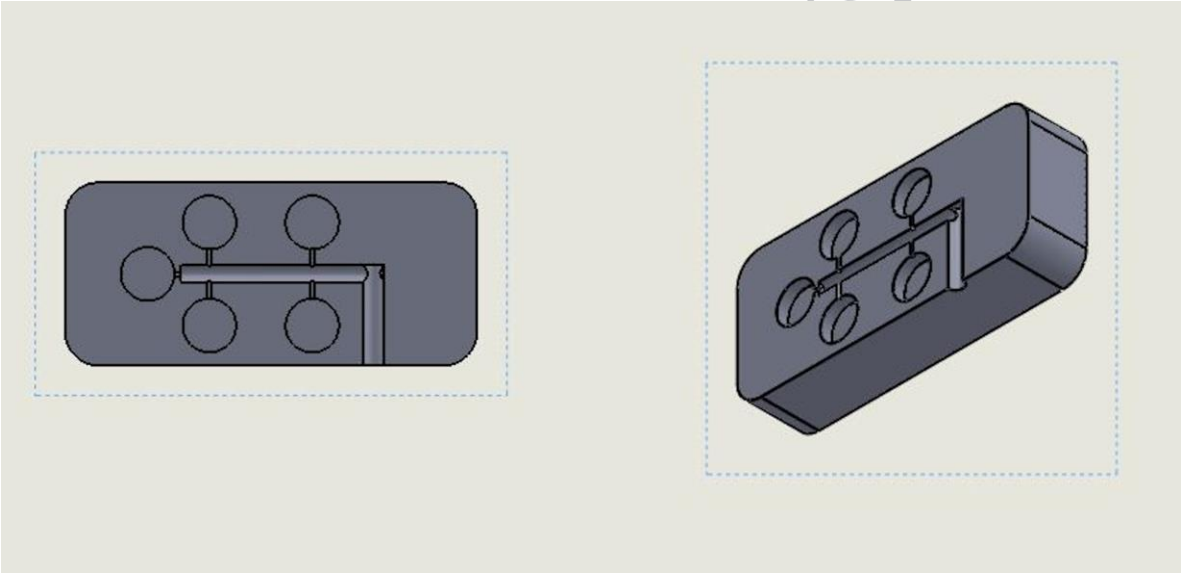

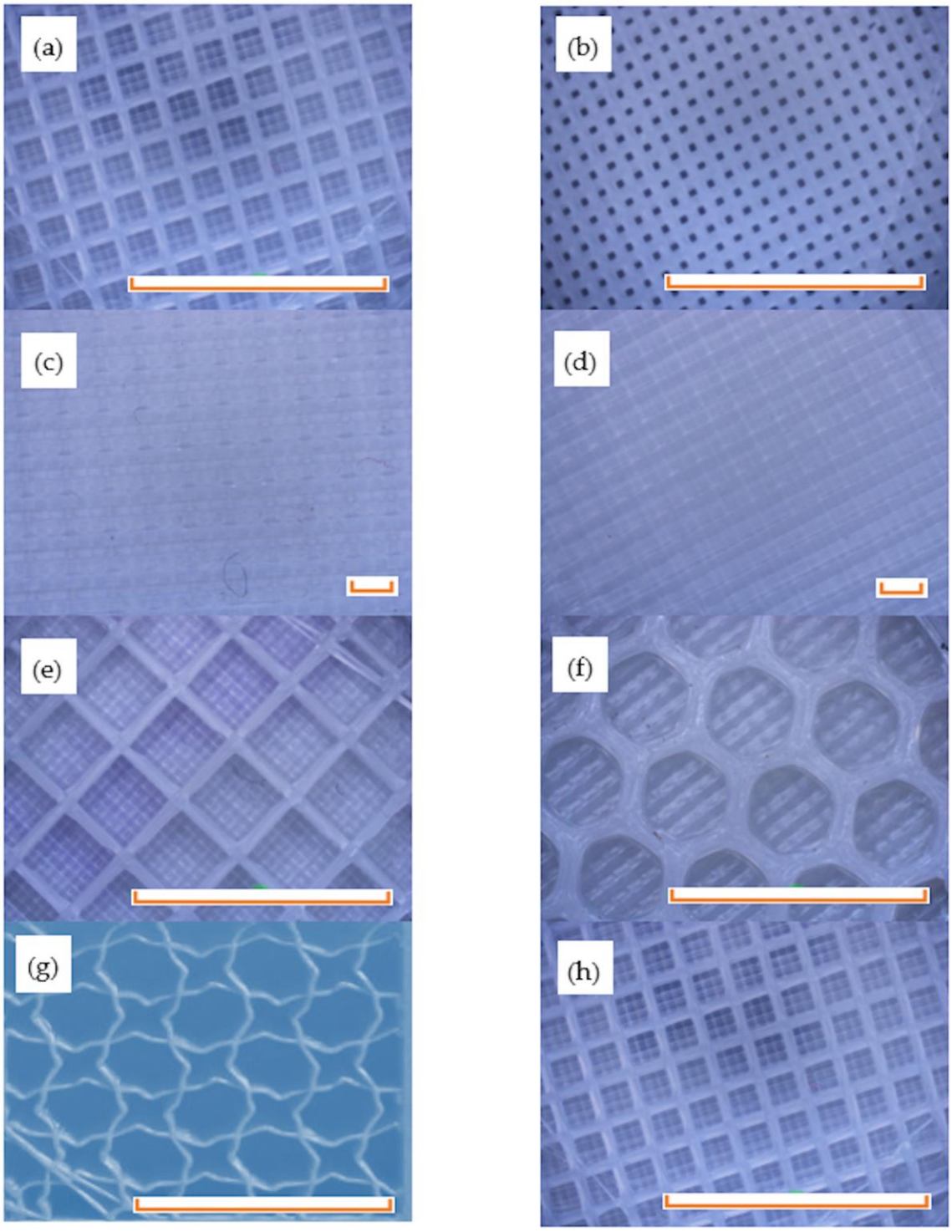

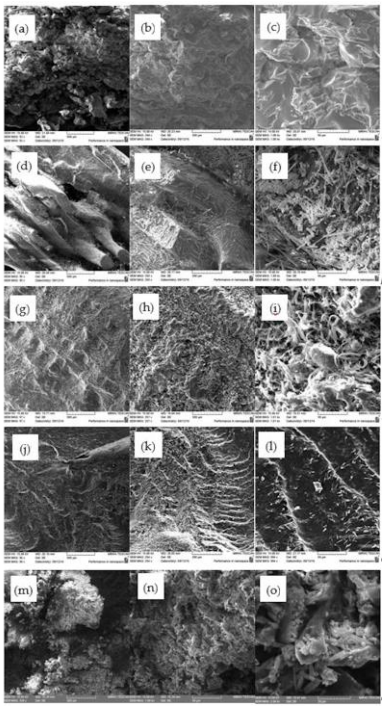

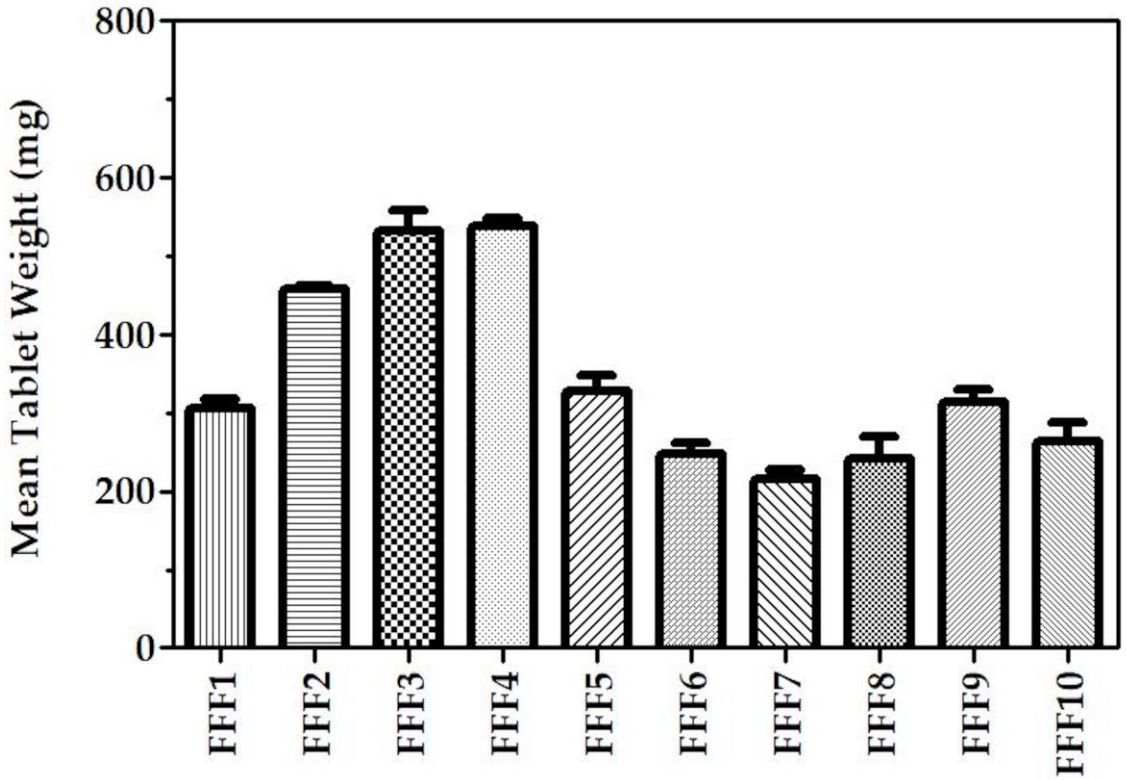

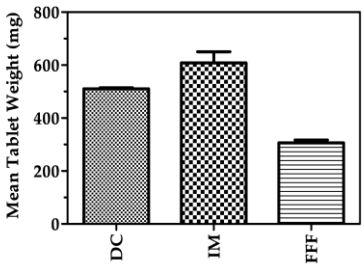

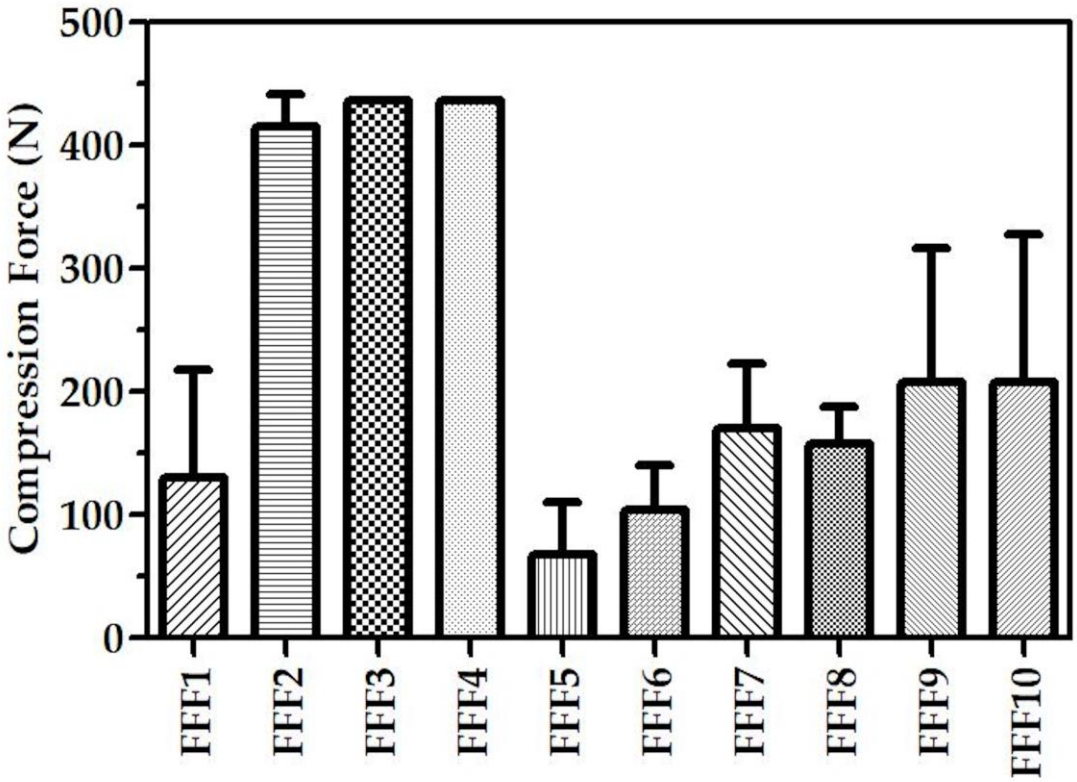

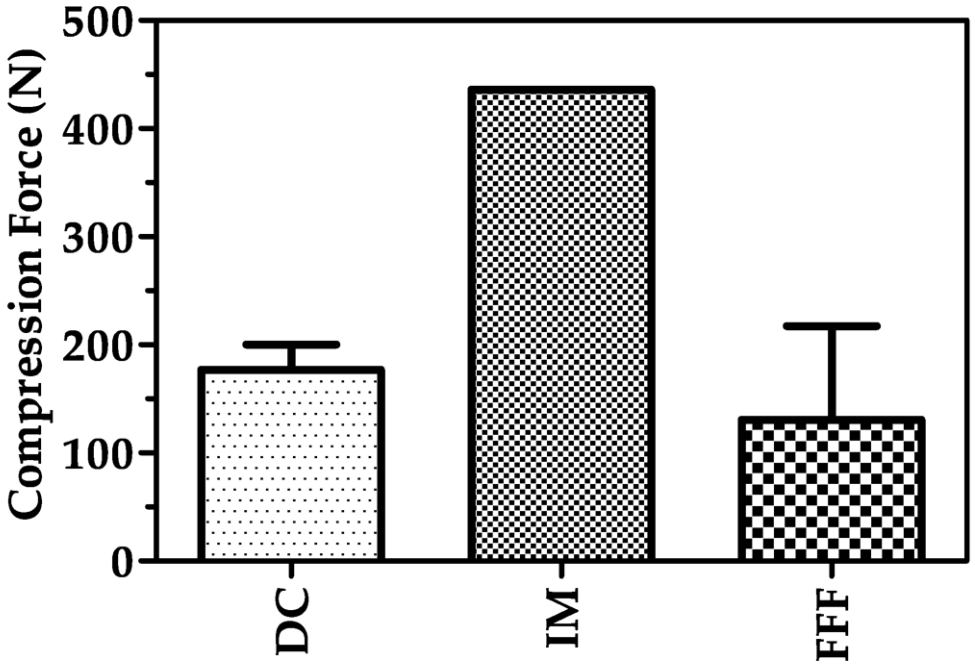

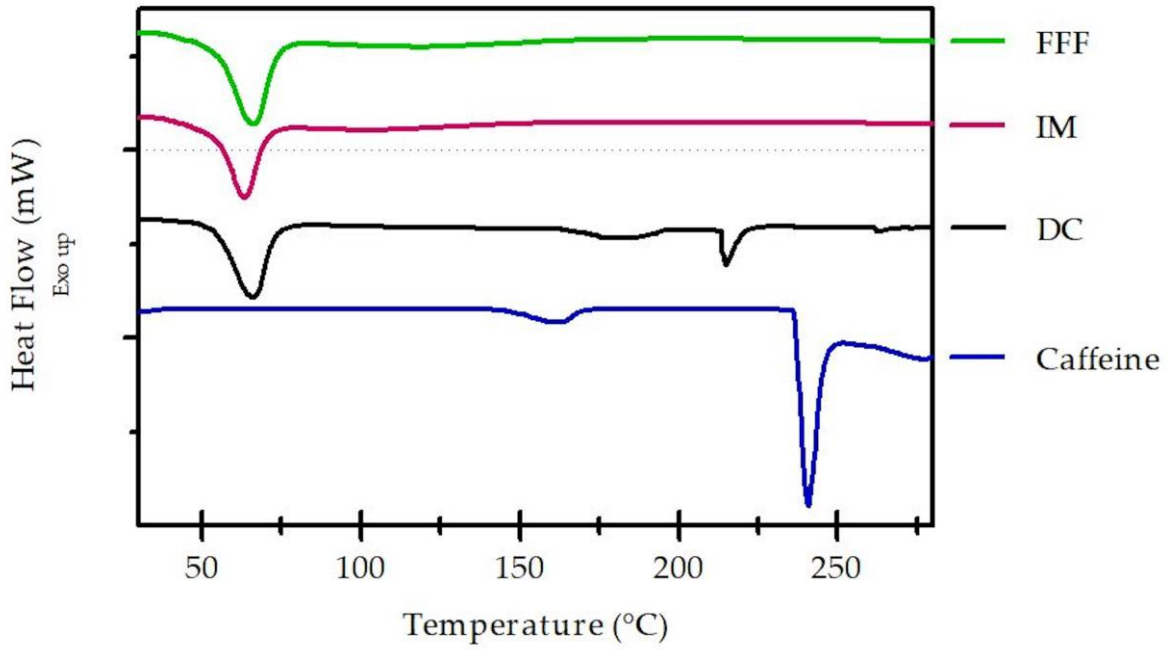

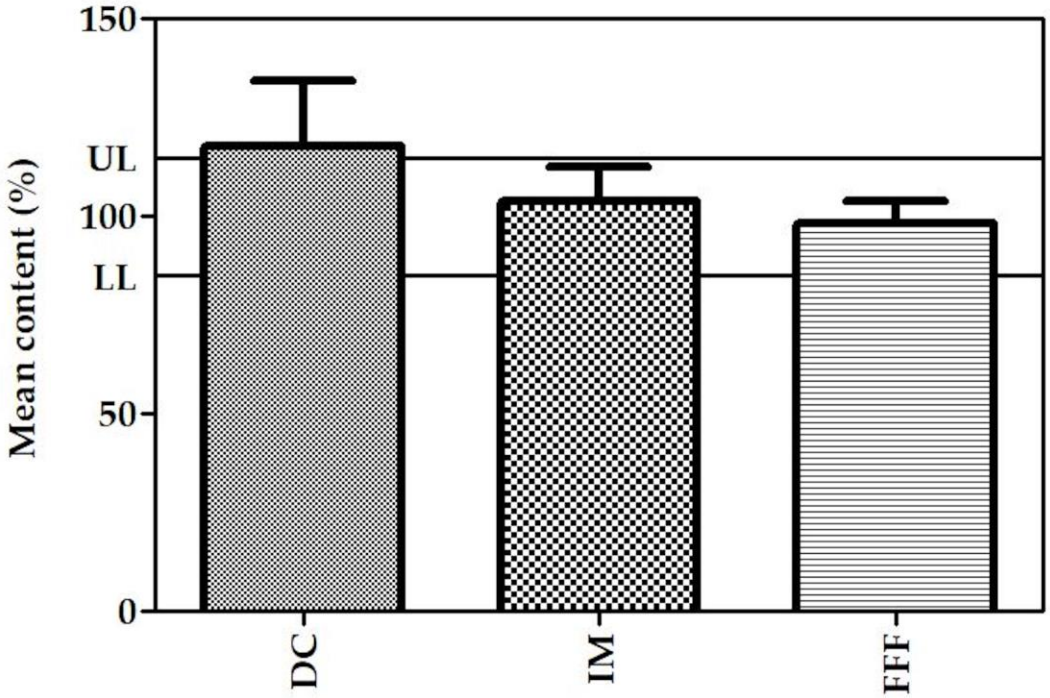

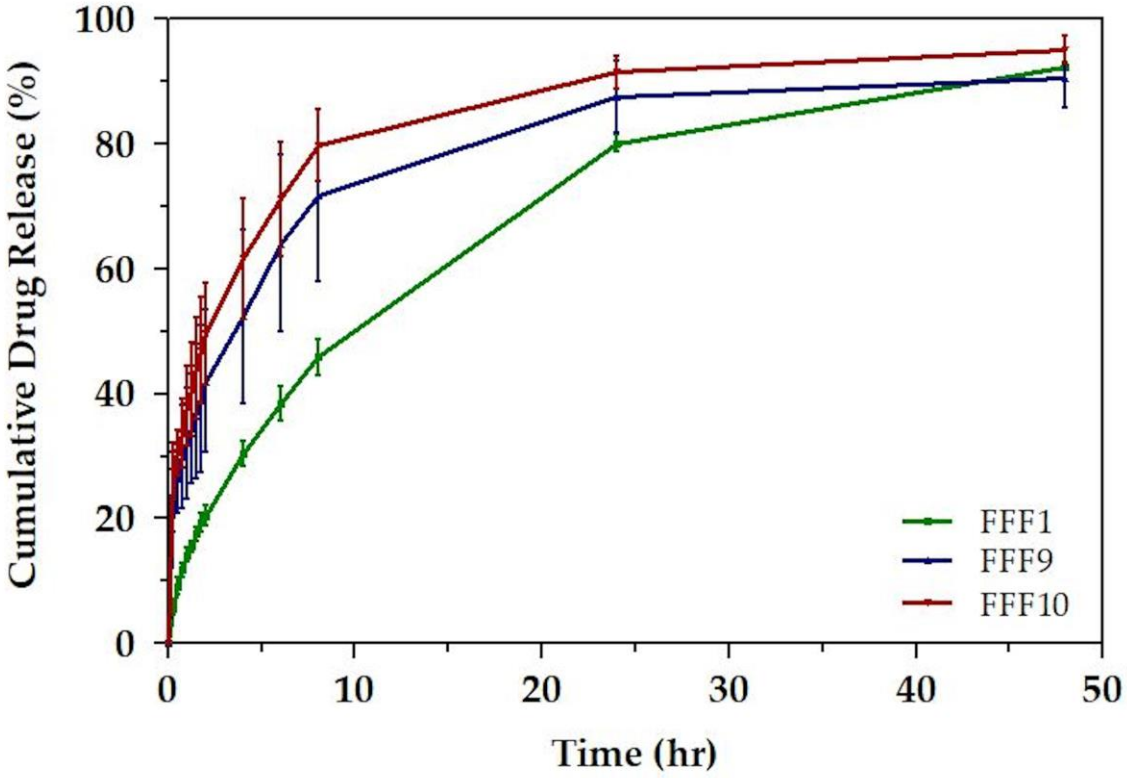

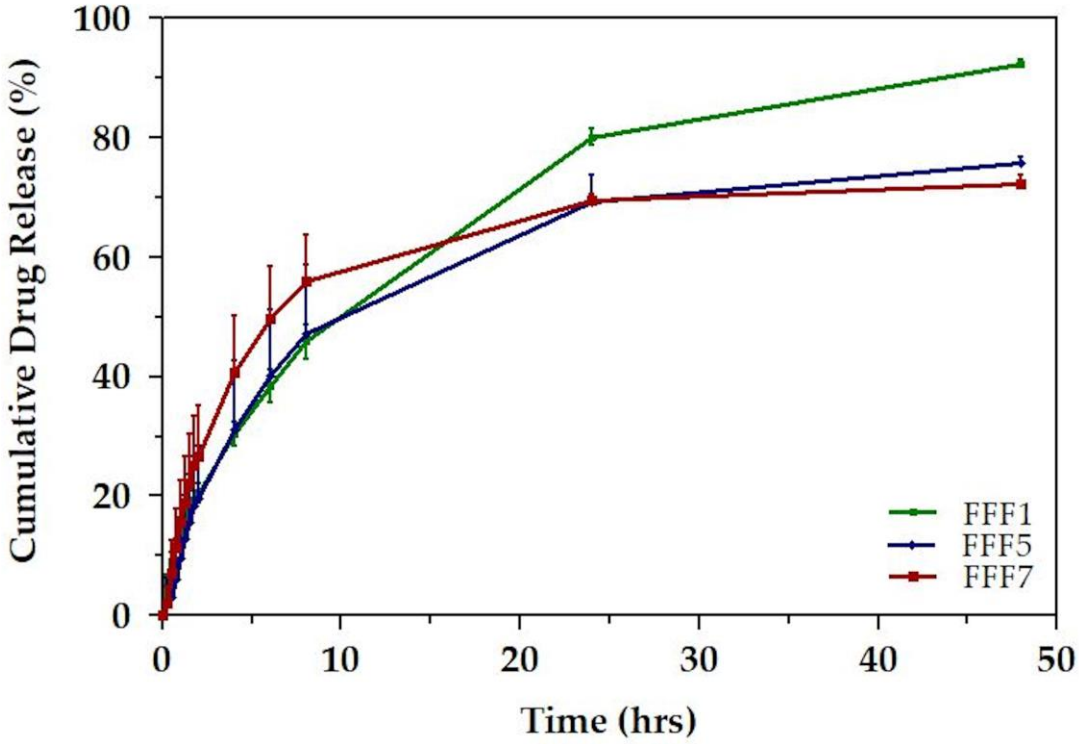

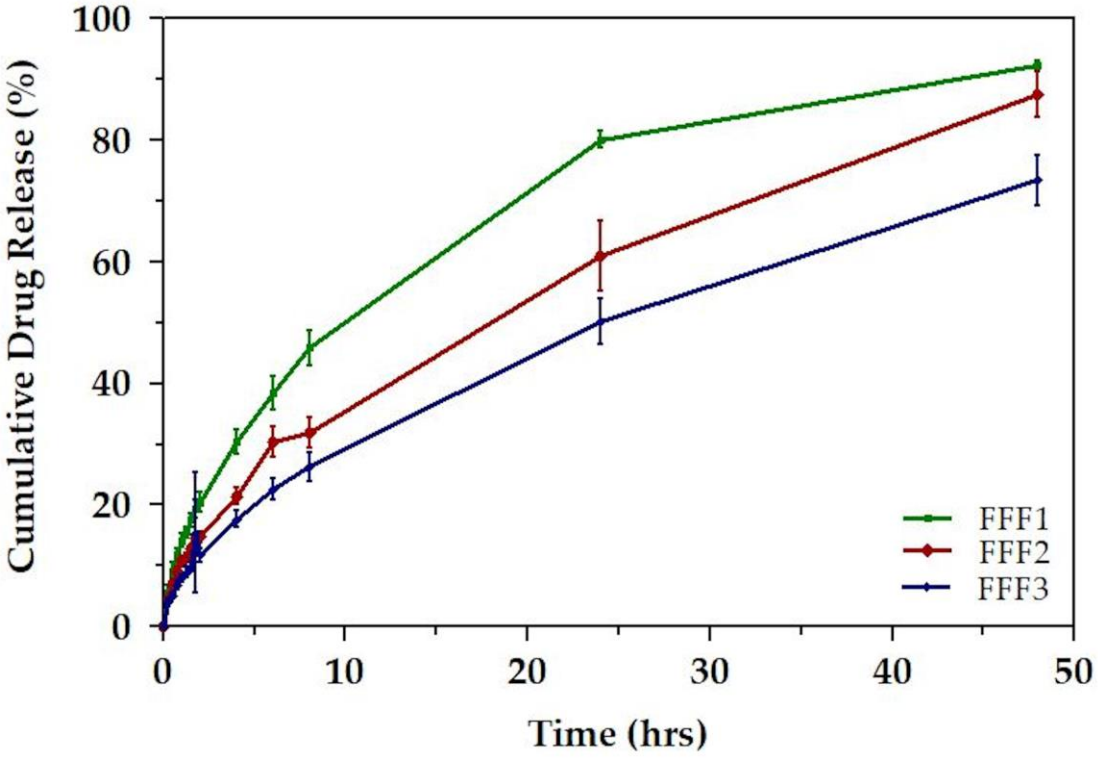

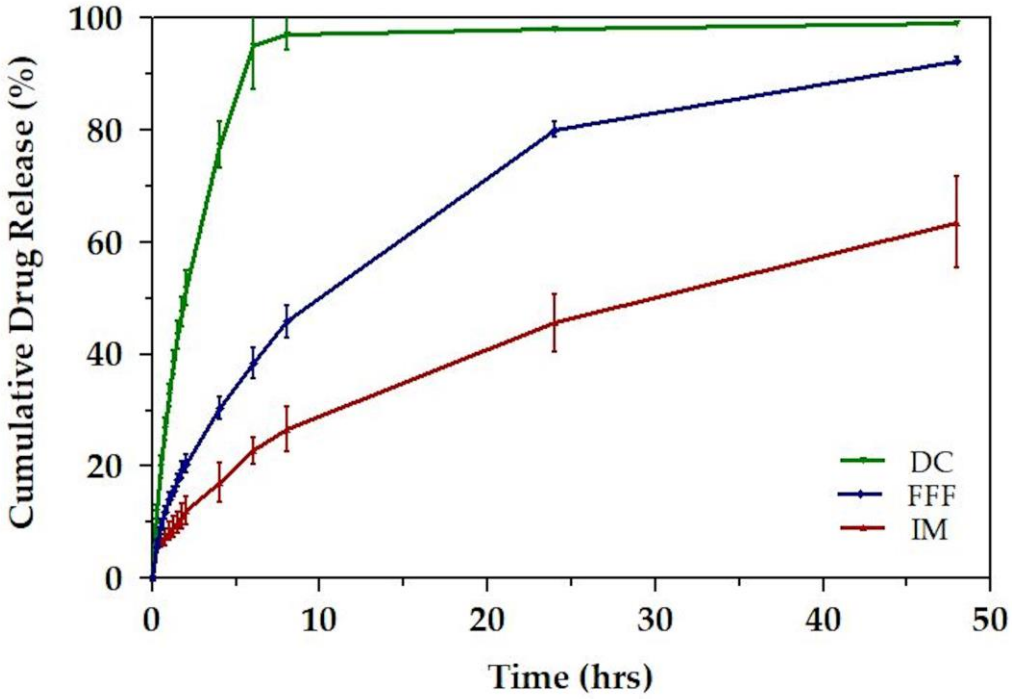

Polycaprolactone
PVP-VA copolymer
Polyethylene oxide
Caffeine

Powder blend

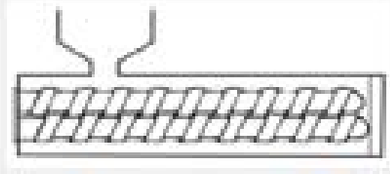

- Direct compression
- Hot-melt extrusion
- 3D printing
- Injection moulding

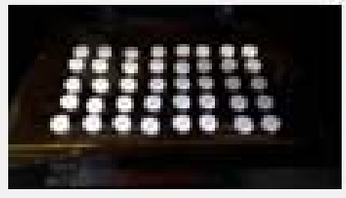

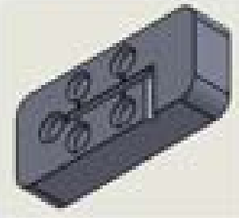

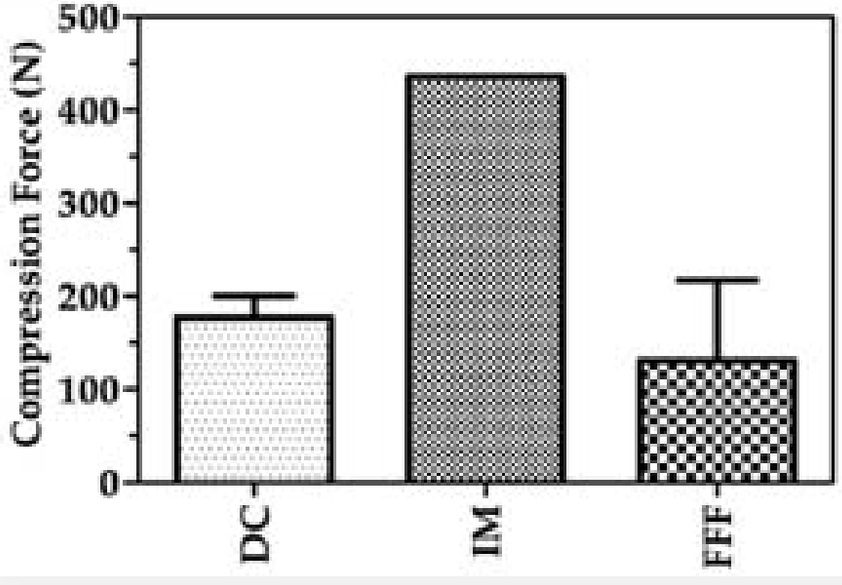


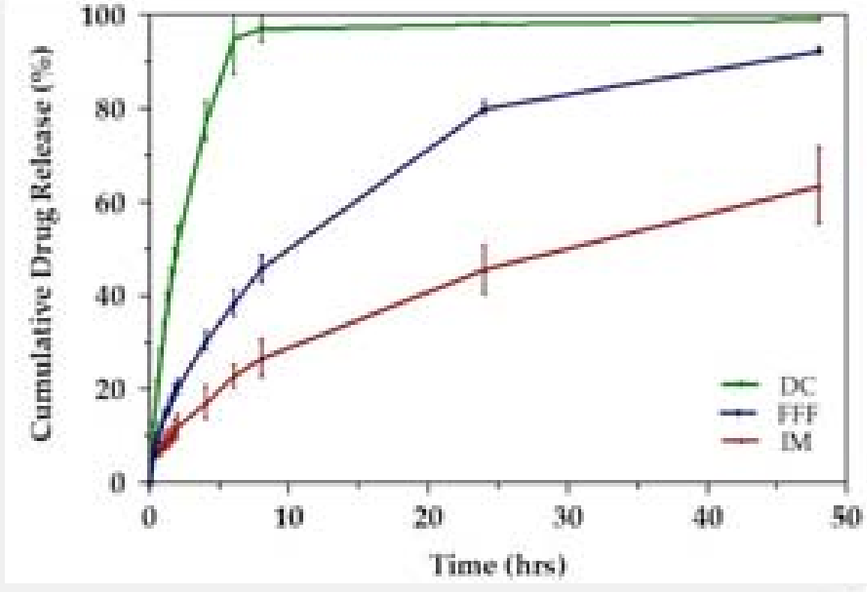

Credit Author Statement:

**Evert Fuenmayor:** Conceptualization, Methodology; Validation; Formal Analysis; Investigation; Data Curation; Visualization; Writing – Original Draft; Writing – Review & Editing

**Martin Forde:** Validation; Investigation

**Andrew V. Healy:** Validation; Investigation

**Declan M. Devine:** Resources; Writing – Review & Editing

**John G. Lyons:** Resources; Writing – Review & Editing; Supervision

**Christopher McConville:** Formal Analysis; Writing – Review & Editing

**Ian Major:** Conceptualization, Methodology; Formal Analysis; Funding Acquisition; Visualization; Project Administration; Supervision; Writing – Original Draft; Writing – Review & Editing